NASA-TM- 20260001558

Radar Performance Characterization Through Correlation with Automatic Dependent Surveillance-Broadcast from General Aviation

Joshua, K., Carbonneau
Metis Technology Solutions, Inc., Hampton, Virigina

Bryan, J., Petty
National Aeronautics and Space Administration Langley Research Center, Hampton, Virginia

National Aeronautics and
Space Administration

Langley Research Center
Hampton, Virginia 23681-2199

April 2026

Available from:

NASA STI Program / Mail Stop 050
NASA Langley Research Center
Hampton, VA 23681-2199

Acknowledgements

The authors would like to thank Lon Kelly from NASA Langley Research Center the Simulation Development and Analysis Branch (D107), Jay Ely from NASA Langley Research Center from the Research Directorate (D3) and Matthew Coldsnow from NASA Langley Research Center UAS Operations Office (D101) for their support in this research project. The authors would also like to thank George Switzer from the Computational Aerosciences Branch (D302) for his help in troubleshooting the scripts early in the development of this project. The authors would also like to thank Charles Liles from D402B for supporting imagery.

Artificial Intelligence (AI) Usage Disclosure: This document was created with assistance from Imagen gen AI model in Google Cloud Platform for generation of background image of circular plots for a higher contrast between the land and water. The content has been reviewed and edited by Bryan Petty. More information on the extent and nature of AI usage is included in the Methods or Acknowledgements sections of the document. https://nasa.sharepoint.com/sites/NASASTIProgram/SitePages/Artificial-Intelligence-(AI)-Guide-for-STI.aspx#ai-usage-disclosure-statement

Table of Contents

List of Figures

List of Tables

Executive Summary

NASA Langley Research Center has several traffic sensors of various types installed around the center to monitor air traffic. These sensors help support beyond visual line of sight (BVLOS) operations. In December 2024, NASA Langley Research Center D107 Simulation Development and Analysis Branch (SDAB) stood up a system to record data from all these sensors. To analyze the performance of these systems, a system of scripts was developed to accept recorded Radar and Automatic Dependent Surveillance-Broadcast (ADS-B) data, correlate these datasets to each other, and measure the difference between the position of the aircraft as reported by the Radar system, and the ADS-B data recorded from the same aircraft. This enables analysis to see where the Radar systems provide adequate coverage of the airspace and where there may be areas of lower precision.

Introduction

This report focuses on ADS-B data recorded from the Longbow Sunhillo ADS-B station, and Radar data recorded from the Lightweight Surveillance and Target Acquisition Radar (LSTAR) and Ground Aware 9120 (GA9120) stations. This combination of sensors is used as a ground based detect and avoid method to conduct BVLOS operations at NASA Langley Research Center in Hampton, Virginia. [1, 2]. Programming scripts were developed to ingest, record, parse and correlate data from these sensors, logging correlated Radar and ADS-B tracks into comma separated value (CSV) files. These CSV files were then parsed by a python script to calculate the total number of correlated data, altitude skew between ADS-B and Radar tracks and averages for azimuth, elevation, range, and distance errors. These results were then translated into table and circular charts to provide a visual representation of the Radar system performance characterization based on range and azimuth from Radar location.

While initial characterization of these sensors was conducted, this report analyzes the performance of these sensors over a longer period. This effort helps refine the NASA Langley Research Center Research Center BVLOS safety case to support more complex missions in air traffic management research, onboard aircraft autonomy research, and center operations, like facility inspections. The range of this analysis covers aircraft detect within 25 Nautical Miles (NM) of NASA Langley Research Center Research Center with altitude being limited by the Radar specification. The scripts developed for this analysis can accept data from any of the traffic sensors installed around the center.

1.0 Radar Stations

1.1 LSTAR

Syracuse Research Corporation's LSTAR model AN/TPQ-49 is a Radar system consisting of an electronically scanned, non-rotating cylindrical phased array antenna. The LSTAR operates in the L-Band frequency range (1-2GHz) and has a field of view of 360 degrees azimuth, and 30 degrees in elevation. The system allows three-dimensional detection of targets within an instrumented range of 40km (~21.6NM). Figure 1 shows an image of the location of the LSTAR characterized in this analysis on top of the NASA Langley Research Center Hanger. Since this is a semi-permanent installation, the Radar is inside a dome for protection. Table 1 shows the manufacturer specifications of the LSTAR, which comes from the User's Manual [3].

Figure 1: LSTAR Installation on NASA Langley Research Center Hangar

Table 1: LSTAR Performance Capabilities

Performance Parameter	Capability
Azimuth Coverage	0 to 360 Degrees
Azimuth Track Accuracy	+/- 0.8 Degrees
Elevation Coverage	30 Degrees
Elevation Track Accuracy	+/- 1.5 Degrees
Instrumented Range	40km or ~21.6NM
Range Track Accuracy	25m or ~0.0135NM

1.2 GA-9120

The GA-9120 is a 3-Dimensional multi-beamforming Radar system operating in the S-Band frequency range (3.0 – 3.3 GHz) with a field of view of 120 degrees in azimuth, and 12.5 degrees in elevation. NASA Langley Research Center has two GA-9120 panels mounted on the gantry in a stacked configuration, with a 90 degrees offset. This gives the system 210 degrees field of view with both panels. The instrumented range of this sensor is from 100m out to 15km (~8.1NM). The Radar facing the south is set at an angle of 5 degrees above the horizon, giving a 95 degrees angle from the ground. Figure 2 shows the installation of the GA-9120 Radars on the Gantry. Table 2 shows the performance specifications for the Radar from the manufacturer. [4] Figure 3 shows the estimated coverage of all Radar systems based on their specifications and locations.

Figure 2: GA-9120 Panels Installed on Langley Gantry

Table 2: GA-9120 Specifications

Performance Parameter	Capability
Azimuth Coverage	120 Degrees per Radar
Azimuth Track Accuracy	+/- 0.25 Degrees
Elevation Coverage	12 Degrees
Elevation Track Accuracy	+/- 0.5 Degrees
Instrumented Range	15km or ~8.1NM for Large Aircraft
Range Track Accuracy	Not specified

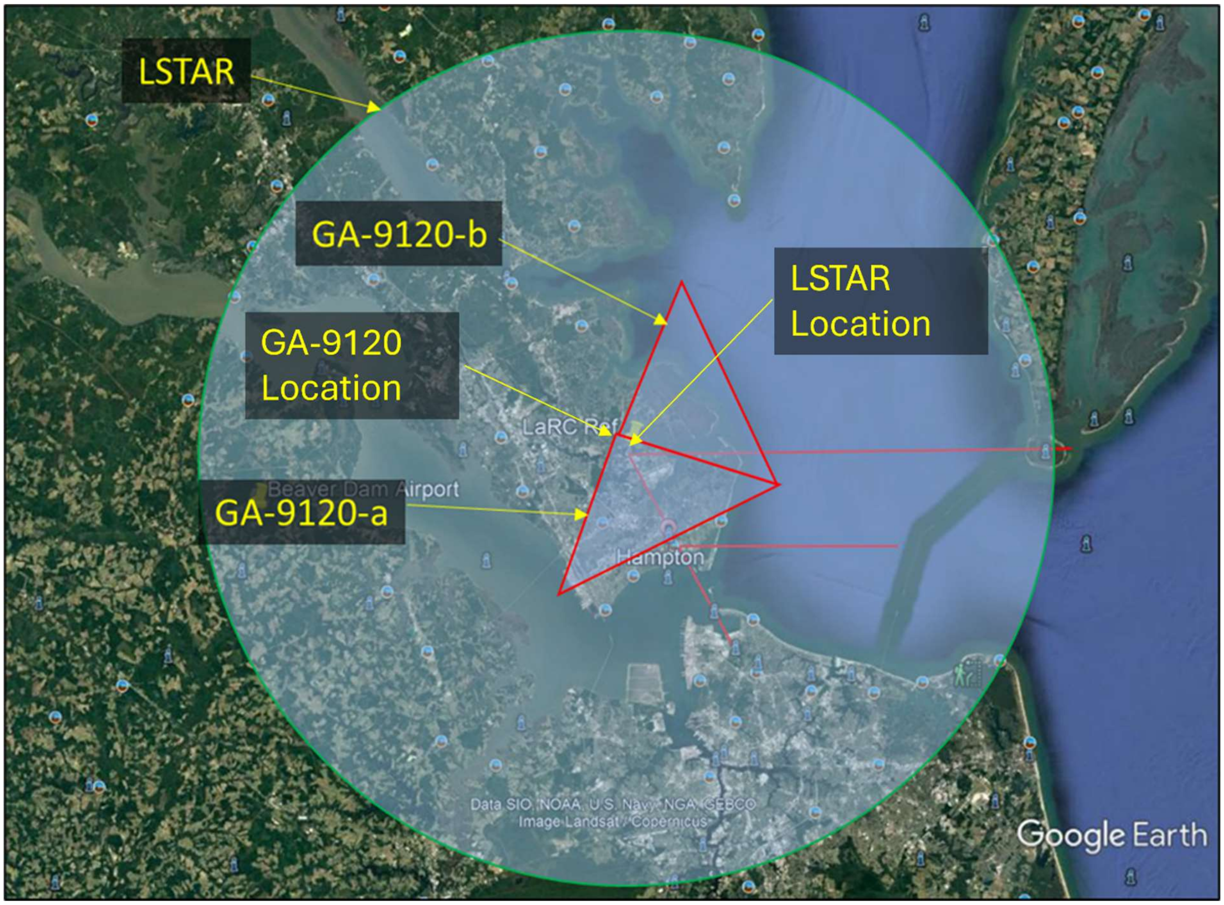

Figure 3: Range and Field of View of the LSTAR and GA-9120 Systems

1.3 Sunhillo ADS-B Receiver

The Sunhillo ADS-B receiver is installed at the Hampton Harbor Center, and receives ADS-B tracks, transmitting them to NASA via a secure Message Queuing Telemetry Transport (MQTT) broker connection. MQTT is a standard messaging protocol for publish and subscribe message transport typically used on remote devices [3]. These ADS-B tracks are recorded alongside the Radar tracks and used later for correlation.

2.0 Recording

2.1 IoRouter

IoRouter is a flexible utility developed by SDAB. It allows routing of data of any type from various inputs to various outputs. Highly configurable, it supports TCP, UDP, MQTT, ZeroMQ, serial, http, and data file formats. The recording system consists of several instances of IoRouter working together to accept data from the Radar and ADS-B sensors around NASA Langley Research Center to record the data in a binary, timestamped format. These files can be played back in real-time in an integrated airspace display called Traffic Awareness and Ubiquitous Real-time Airspace (TAURAS) for traffic simulation. TAURUS allows the researchers to visualize real-time and historical traffic data.

2.2 Distributed Simulation Hub

The Distributed Simulation Hub, known as the distributed_sim_hub, is a utility developed by SDAB to facilitate communication between multiple Langley Standard Real-time Simulation in C++ (LaSRS++) simulations, as well as previously recorded and live Radar data. A distributed_sim_hub instance listens for connections on a specified port, and distributes any messages received from one client to all other connected clients.

2.3 Certain Input/Output Concentrator (CertainIOC)

The data is processed by a central server, named CertainIOC , running on a computer located in NASA Langley Research Center building 1268A running Ubuntu 20.04 Symmetric Multi-Processing (SMP). This host is used to accept data from the traffic sensors around the center, record it, and convert it to VehicleState format for use by various MQTT based applications, including TAURAS. VehicleState holds information on the Radar or ADS-B source of the track, GPS position reported by the source, and state of the track, including speeds. This format can be seen in Table 3. The recording and distribution system consists of several interlinked instances of IoRouter as described in Section 2.1. An overview of the entire system setup can be seen in Figure 4. The following scripts start these instances:

- ***start_all.sh*** – This script is the entry point and runs all the subsequent scripts listed below.
- ***kill_all.sh*** - This script is run prior to any other script to kill any running io_router processes from previous calls. It calls 'killall -INT io_router' first, which sends an interrupt signal to all active io_router processes, shutting them down in a controlled fashion. After five seconds, it then calls 'killall -KILL io_router' to forcibly end any remaining processes that may not have shut down. This final call to killall ends any lingering script processes that are part of the data recording and routing system.
- ***run_hub.sh*** - Checks to see if distributed_sim_hub is running and starts that process if it's not.

2.3.1 VehicleState Structure

Table 3: Vehicle State Data Structure

Field Size (Bytes)	Field Type	Field Name
8	TypeCode(uint8)	type_code
8	uint8	sensor_id
16	unsigned int	participant_address
variable	std::string	callsign
32	double	latitude_deg
32	double	longitude_deg

32	double	altitude_ft
32	double	ground_speed_kts
32	double	track_deg
32	double	vertical_rate_fpm
16	unsigned int	num_custom_fields
variable	float[]	custom_fields

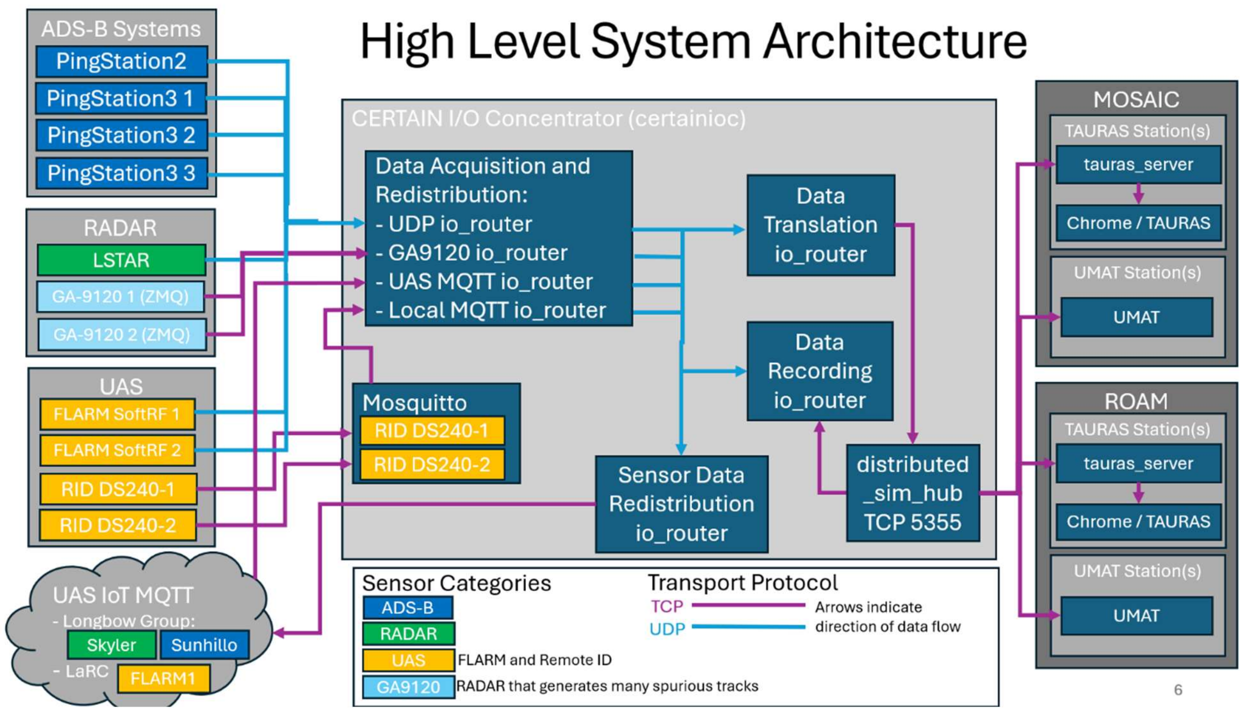

Figure 4: Diagram of the overall system architecture

The following seven scripts all use a similar methodology. Calls with Unix commands “ps” and “grep” are used to determine if an instance of io_router with the required configuration is already running. If one is found, it is killed before a new instance is started.

- ***run_udp_sensors.sh*** –Starts an io_router instance configured to accept data over UDP and route them to various ports. These port numbers are generated by sensor_ports.sh.
- ***run_larc_radar_ga9120.sh*** – Starts an io_router instance configured to use the “zeromq” option of io_router to accept data from the GA9120 Radar system, routing this data to a relay port and a recording port.
- ***run_mqtt_uas_sensors.sh*** – Starts an io_router instance configured to subscribe to MQTT topics containing information from the Longbow Sunhillo ADS-B system, Longbow Skyler Radar system [5], and FLARM data [6].

- ***run_mqtt_local_sensors.sh*** – Starts an io_router instance configured to receive data from an MQTT broker, subscribing to topics containing data from the DroneScout 240 Remote ID receiver.
- ***run_recordings.sh*** – Starts an io_router instance that accepts data on all sensor recording ports associated with previously started io_router instances. The data on each one of these ports is written to a timestamped and flat file.
- ***run_translations.sh*** - Runs an instance of io_router configured to accept data from the relay ports and translates the data into the VehicleState format for use by NASA airspace displays, like TAURAS and the UAS Mission Analysis Tool (UMAT).
- ***run_forwarding_relays.sh*** – Starts an io_router instance that accepts data on all debug ports for each instance of io_router started in the preceding scripts and sends it to the NASA UAS Internet of Things (IoT) MQTT broker.

2.4 Recording File Format

The system of io_router instances results in two types of data files per sensor: Timestamped, and Flat. The format of both types of files is the same, except the Timestamped files contain an elapsed time in seconds at the beginning of each record, to aid in real-time playback.

2.4.1 Timestamped File Format

Table 4: Timestamped File Formats

Timestamp	Record Size	Record Body
32-bit float	16-bit unsigned int	Record Size bytes

Table 4 shows how the timestamped files are stored in memory and their associated sizes. The record body consists of an Asterix record with the type of Asterix depending on which sensor the data came from. For example, the Sunhillo ADS-B sensor uses Asterix 021 messages while the LSTAR uses Asterix 048 messages [7].

2.5 Recording File Archive

The raw data for each sensor is archived weekly on the Langley Central Storage System (CSS) [8]. The files are located in a folder labelled “certain_radar_recordings”, with a separate directory for each sensor for which data is recorded. Files are compressed in zip format for each day with the following file path structure:
/certain_radar_recordings/<sensor_name>/<year>/<month>/<sensor-name>_<month>_<day>_<year>.zip.

3.0 Correlation

Correlation occurs over numerous scripts processing the data, removing data that is not of interest, then comparing remaining ADS-B and Radar data to find the matching tracks. The overview of this process can be seen in Figure 5.

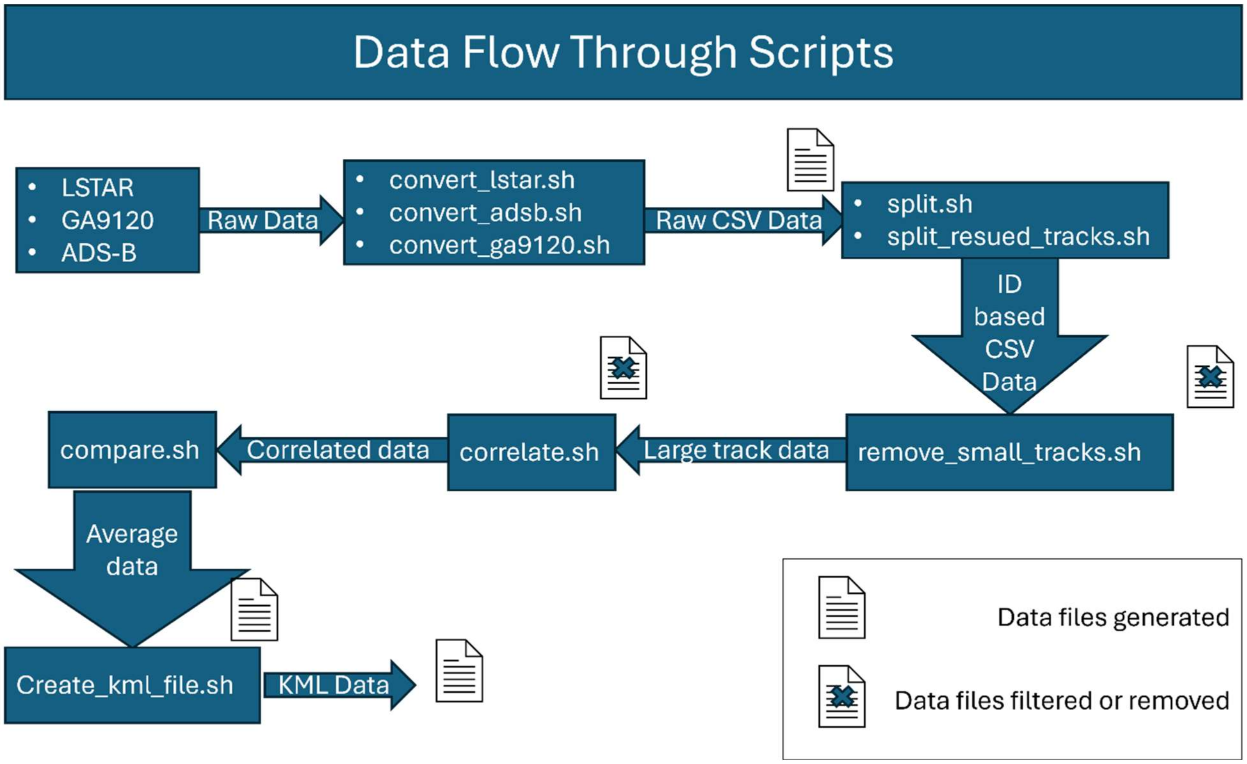

Figure 5: Data Flow Through Scripts

3.1 Scripts for Radar and ADS-B Conversion

These scripts utilize a modified version of io_router to convert the recorded Radar, ADS-B, and GA9120 files to a csv format. The scripts are called *convert_lstar.sh, convert_adsb.sh, and convert_ga9120.sh* that process the LSTAR, ADS-B and GA9120 data, respectively. Each time one of these scripts is run, an instance of io_router starts to playback the input data file. The output data is written to a CSV file instead of routing the information to TAURAS. To speed up writing to the CSV, the playback speed multiplier was set to 100 instead of playing back in real time.

3.2 Scripts to Split Data by ID

This script, called *split.sh*, takes the files from the conversion scripts and calls the Unix commands “awk”, “sort”, and “uniq” to get all the unique track identifiers (IDs), which is column four of the input files. Then, for each track ID, the script uses “grep” to extract all the points associated with that ID and redirects them to a separate CSV file named based on the ID.

Occasionally, the LSTAR will reuse track IDs within a 24-hour period, which results in multiple aircraft with the same track ID. This is possible because track IDs are incremented when a new track is discovered. If enough tracks are registered within a 24-hour time, there is a chance that an ID is repeated. To address this, the Perl script *split_reused_track.pl* parses each track file in the given directory, looking for gaps in the timestamps of sufficient length that would indicate another track was created with the same ID. By default, this threshold is 1000 seconds, which is about 17 minutes. When such a gap is encountered, the script generates new files for each separate track that was contained in the track file, with a number appended to the end of the track ID. For example, a track file named aaa.csv that contains three time-separated tracks will be split into three files: aaa0.csv, aaa1.csv, and aaa2.csv.

3.3 Script to Filter of Short Duration Tracks

The script *remove_small_tracks.sh* is a simple shell script that calls the Unix commands "head" and "tail" to get the first and last lines of each file in the given directory. The command "awk" is then used to extract the timestamps from column one of the first and last line and subtracts them to get the total length of the track. If this is less than 30 seconds, which is configurable based on user requirements for correlation, the track file is deleted.

3.4 Script to Correlate ADS-B and Radar Tracks

The correlation script, *correlate.*pl, is the most complex and time-consuming step of the process. It takes a single Radar track file and a file containing all the ADS-B tracks to be searched for correlation. Starting at the beginning of both files, each line is tokenized to extract the timestamp, latitude, longitude, and altitude. First, the timestamps are compared. If the Radar timestamp is more than 0.5 seconds ahead of the ADS-B timestamp, the script will skip to the next line of the ADS-B file. If the Radar timestamp is more than 0.5 seconds behind the ADS-B timestamp, the script will skip to the next line of the Radar file. This allows the script to parse through both files looking for timestamps that line up within half a second, indicating correlation. When two lines with close timestamps are found, the difference in the latitudes, longitudes, and altitudes are used to determine the rough distance between the two points. Comparison of the difference in latitude and longitude are used directly, instead of a more complicated great circle distance calculation, to keep the runtime of this script as low as possible while still providing a good estimate of if the tracks are near each other. When two points are found that have a latitude and longitude difference within 0.005 degrees and altitudes that are within 1000 feet, the two tracks are considered correlated. The script stops comparing the two files and prints the two track IDs to standard output. In use, this output is redirected to a file and a list of correlated track ID pairs is generated after this script runs on every Radar track in the dataset. Both the LSTAR and GA9120 data are correlated using the same method.

3.5 Script to Compare and Calculate Averages

Next, the *compare.pl* script is used to do several calculations on each track pair that was correlated in the previous step. Like the correlation step, both the Radar and ADS-B files are parsed, line by line, until the timestamps are within 0.5 seconds. After this alignment procedure, the great circle distances are calculated between the Radar station location and both the Radar and ADS-B points. These distances will be used to calculate the elevation angle from the Radar station. The script also calculates the azimuth angle of both points in relation to the Radar station location. The ADS-B data is treated as truth for aircraft location, so the Radar azimuth subtracted from the ADS-B azimuth is the azimuth error. Likewise, the Radar elevation subtracted from the ADS-B elevation is the elevation error. To avoid large azimuth error values when the Radar and ADS-B azimuth values are on either side of 0 degrees, the script checks if the azimuth error or the absolute value is greater than 358 degrees, which indicates a target near the north. If so, the calculation is adjusted accordingly so it reflects the correct difference between the angles. While the script is calculating these errors, it is also keeping track of the maximum azimuth and elevation errors and the ADS-B azimuth and elevation when these maximum errors occurred. These values are written to the average.csv file after the files have been fully processed, along with the Mean and Root Mean Square of the azimuth and elevation errors, and the Mean of the latitude, longitude, and altitude of the track section that was compared.

3.6 Script to Generate KML Data create_kml_file.pl

The last step is to create a KML file containing the tracks for visualization using the *create_kml_file.pl* script. The KML creation script simply takes the list of track pairs created by the correlation script and parses the latitude, longitude, and altitude of each point for each track, outputting the points into a KML file that can then be loaded into Google Earth to see the tracks. The KML file will contain two paths, one for the ADS-B data and one for the Radar track. Figure 6 shows an example of this visualization where the blue is an ADS-B track and the red is the correlated Radar track.

Figure 6: Visualization of Correlated LSTAR Track via Google Earth

3.7 Output File Structure

Data from each day is stored in its own directory, in the format YYYY-MM-DD. An example of the directory for February 2nd, 2025, can be seen in Figure 7. The directory contains the following files:

- ***<sensor>_timestamp_recording_yyyy-mm-dd.csv*** – Contains every data point recorded from the given sensor for the day. Each line contains the following data: timestamp (seconds since midnight UTC), message type code, sensor ID, track ID, aircraft callsign, latitude, longitude, altitude (feet), airspeed (knots), ground speed (knots), heading (degrees), track (degrees), vertical speed (feet per minute), custom field 1, custom field 2 and custom field 3. Depending on which sensor the data originated from, some fields may not be used. The directory contains one of these CSV files for the LSTAR, Sunhillo, and both GA-9120 units.
- ***<sensor>_timestamp_recording_yyyy-mm-dd*** – Directory containing a separate CSV file for each track recorded by the sensor on that day. The format is the same as the files described above. The filenames are of the format <track-id>.csv.
- ***<sensor>_correlated.txt*** – File containing the correlated track pairs from the given sensor. Each line contains a pair of track IDs, separated by a comma, in the format <Radar ID>,<ADS-B ID>.
- ***<sensor>_compared*** – Directory containing one CSV file for each correlated track pair. These files contain a point-by-point comparison of the Radar and ADS-B tracks. For each point, there's a line containing the following information: Radar Track ID, ADS-B Track ID, Aircraft Callsign, Radar Timestamp, ADS-B Timestamp, Timestamp Difference, Radar Latitude, Radar Longitude, Radar Altitude (ft), ADS-B Latitude, ADS-B Longitude, ADS-B Alt (ft), Radar Range (NM), ADS-B Range (NM), Range Error, Radar

Azimuth (Degrees), Radar Elevation (Degrees), ADS-B Azimuth (Degrees), ADS-B Elevation (Degrees), Azimuth Error and Elevation Error. In addition to these individual files, this directory also contains an average.csv file, which contains the average calculations made on each track in the directory. For each correlated track pair, this file contains: Radar Track ID, ADS-B Track ID, Aircraft Callsign, Average Range (NM), Mean Azimuth Error (Degrees), Mean Elevation Error (Degrees), RMS Azimuth Error (Degrees), RMS Elevation Error (Degrees), Maximum Azimuth Error, Azimuth at Maximum Azimuth Error, Elevation at Maximum Azimuth Error, Maximum Elevation Error, Azimuth at Maximum Elevation Error, and Elevation at Maximum Elevation Error. This data allows for an overall look at each correlated Radar track on a specific day and gives an idea of how closely it matches the ADS-B data.

Name	Date modified	Type	Size
ga9120_1_compared	9/22/2025 12:24 PM	File folder	
ga9120_1_timestamp_recording_2025-02-13	9/22/2025 12:24 PM	File folder	
ga9120_2_compared	9/22/2025 12:24 PM	File folder	
lstar_compared	9/22/2025 12:24 PM	File folder	
lstar_timestamp_recording_2025-02-13	9/22/2025 12:16 PM	File folder	
sunhillo_timestamp_recording_2025-02-13	9/22/2025 12:17 PM	File folder	
ga9120_1_correlated	9/15/2025 1:33 PM	Text Document	1 KB
ga9120_1_timestamp_recording_2025-02-13	9/15/2025 11:50 AM	Microsoft Excel Com...	14,295 KB
ga9120_1_tracks_2025-02-13.kml	9/15/2025 2:30 PM	KML File	717 KB
ga9120_2_correlated	9/15/2025 2:30 PM	Text Document	0 KB
ga9120_2_tracks_2025-02-13.kml	9/15/2025 2:30 PM	KML File	1 KB
lstar_correlated	9/15/2025 12:11 PM	Text Document	1 KB
lstar_timestamp_recording_2025-02-13	9/15/2025 11:18 AM	Microsoft Excel Com...	3,582 KB
lstar_tracks_2025-02-13.kml	9/15/2025 2:30 PM	KML File	14,119 KB
sunhillo_timestamp_recording_2025-02-13	9/15/2025 11:34 AM	Microsoft Excel Com...	82,632 KB

Figure 7: Example of Output File Structure

4.0 Analysis of Correlated Data

After the data has been organized into CSV files by date and sensor type, the team did a deeper analysis of the information. This includes looking at the average values of azimuth, elevation, altitude, lateral distance and range error. Each of these values are looked at over a results grid of 25 x 36 based on the distance in nautical miles and bearing in degrees from the location of the Radar. The total number of tracks used for calculations in each cell are also looked at to show where most correlated tracks are. The team also determined the percentage of times that the Radar track altitude was below the ADS-B track altitude showing where the Radar typically skews low on altitude. Data presented in this report will cover nine months from January 1st, 2025 to September 30th, 2025. This data only represents "targets of opportunity" that are captured by the Radars while emitting their ADS-B position and does not include non-emitting aircraft.

4.1 Preprocessing of Data

Prior to including a data point into the final averages, filters on azimuth, range, latitude, longitude and altitude were applied to ensure that the correlated data point is accurately correlated. This filter helps ensure that any points captured in the correlation that are not correlated when compared are removed. This may have occurred due to the ID labeling of the Radar systems not syncing with the ADS-B IDs throughout the track history. All filter values chosen were intended to remove large error values, but not to remove valid correlations. Tracks were filtered on five criteria: azimuth error, range error, latitude and longitude difference and an altitude range. Each error was checked in that order. For example, if a track is removed in the azimuth check, it is not checked by the remaining filters. Figure 8 shows how data from scripts is filtered out by each filter and what data is eventually used in the analysis.

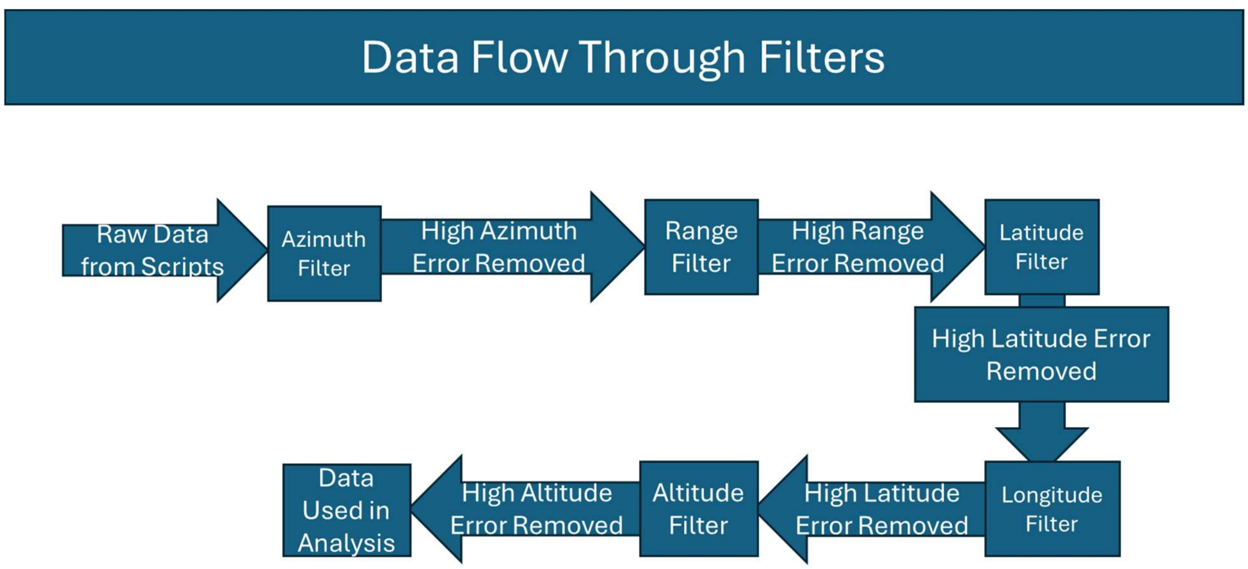

Figure 8: Data Flow Through Filters

Azimuth error was pulled directly from the CSV files and compared to the azimuth filter, which was set to +/- 10 degrees. This removed all points where the difference in azimuth between the Radar track and ADS-B track were more than 10 degrees in either direction. Similarly, the range error was pulled from the CSV files and tracks outside of a range of +/- 1NM are removed from the calculations. Latitude and longitude differences were calculated based on ADS-B and Radar values from the CSV files. The filter for latitude was 1E-2 degrees while the filter for longitude is 12E-3. At the location of the Radar systems, this is around 1.112km and 1.066km of lateral distance for latitude and longitude respectively. If the absolute value of the difference between the Radar and ADS-B track were larger than the filters, those points are removed from consideration. The final filter was altitude which removed all tracks where the altitude of the ADS-B was above 90,000ft or below zero. Table 5 shows the filter types, the range of the filter values and the total number of tracks removed from the different Radars based on the filter.

Table 5: Data Removed by Data Filters

Filter Type	Filter Value	Data Points Removed from LSTAR data set	Data Points Removed from GA9120 data set
Azimuth	+/- 10 Degrees	34303	49449
Range	+/- 1NM	11231	6834
Latitude	+/- 0.01 Degrees (~1.112km)	15420	2421
Longitude	+/- 0.012 Degrees (~1.066km)	10240	3775
Altitude	0 to 90000ft	21588	2030

The filters removed a total of 92,782 out of 4,771,450 possible tracks from the LSTAR and 64,509 out of 181,156 possible tracks from the GA9120 files. This resulted in 4,678,668 tracks being used from the LSTAR and 116,647 tracks being used from the GA9120. The filters removed 1.955% of the correlated track from the LSTAR data set while 35.61% of the tracks from the GA9120 dataset, largely due to azimuth error.

4.2 LSTAR Analysis

Because of the LSTAR's 360-degree field of view and instrumented range of 40km (or ~21.6NM), the ranges used in the analysis for both Radars will be 0 degrees to 360 degrees of azimuth and out to 25NM. These values will be relative to the location of the Radar since the correlated data is based on that location. A step of 10 degrees azimuth and 1NM for the range from the Radar was used, creating the 25 x 36 results grid. While data was collected from January to September, there was a filter applied the range of data capture prior to July, which limited tracks coming out of the Radar to 10NM. This filter was due to the configuration of the LSTAR for operations to limit the tracks that appeared on displays. The filter was identified in July and removed for data captured after to fully evaluate the system.

4.2.1 LSTAR Total Points

Figure 9 shows a heatmap representation of the distribution of targets used during this analysis. The X-axis represents the distance from the Radar in NM, and the Y-axis is the bearing range from the Radar, with 0 being true north. Values are based on the ADS-B location of the correlated track. There are two main pockets of traffic within this figure. The first one is around 5NM to 6NM out at 300 degrees to 310 degrees, which aligns to the approach and departure flight paths of Newport News International Airport (PHF). The second is around 14NM to 15NM at a bearing between 140-150 degrees, which lines up with the Norfolk International Airport

(ORF). There is also a small cluster between 2NM and 7NM at 70-80 degrees bearing which lines up with the departure path of Langley Air Force Base over the Back River towards the Chesapeake Bay. There is likely less density in this area due to the increased amount of non-ADS-B emitting military traffic. Figure 9 also shows how traffic within 2NM of the Radar is much less dense, likely due to the 30-degree elevation angle and restricted Class D airspace of Langley Air Force Base. This results in an area above the LSTAR that tracks are not seen, which is referred to as the "cone of silence" and limits the traffic seen to roughly 7,000ft and below at 2NM out and roughly 3,500ft and below at 1NM out.

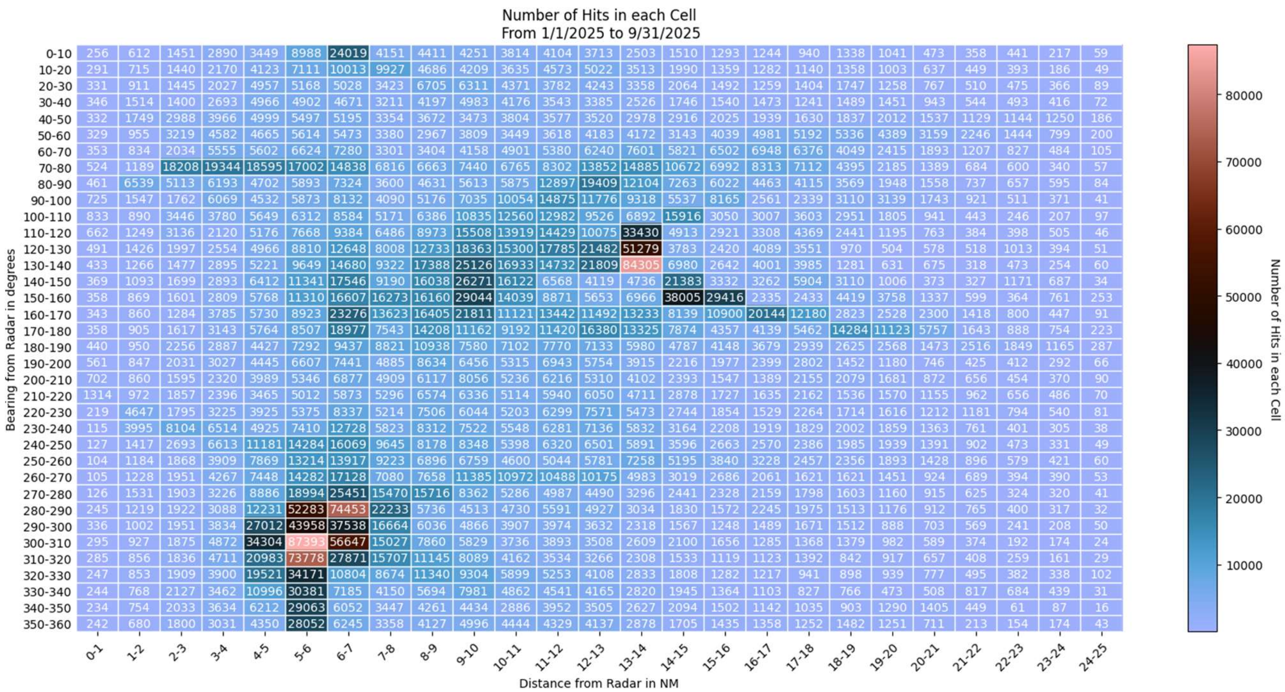

Figure 9: Total Number of Hits of LSTAR

4.2.2 LSTAR Average Azimuth

Figure 10 shows a heatmap based on the average azimuth error between the correlated Radar and ADS-B tracks. This value was pulled directly from the CSV files, summed based on each cell, and averaged based on the number of hits in that cell. Since the azimuth error is calculated by subtracting ADS-B azimuth from the Radar azimuth, positive values result in Radar target skew counterclockwise and negative values skew clockwise. The resulting heatmap shows that most of the values fall within the +/-0.5 degrees of azimuth error with some higher errors on the 90 degrees to 130 degrees, 180 degrees to 190 degrees and 230 degrees to 330 degrees range. Notably, there are large errors within 1NM of the Radar, however this is likely due to the aircraft being closer and even small lateral distances between the ADS-B track and Radar track will result in a larger azimuth. The LSTAR Radar's instrumented azimuth accuracy on detections are 1.25 degrees and 0.8 degrees on tracks according to the SRC LSTAR Manual [3]. Data provided to the correlation scripts are track only, meaning even with stricter requirements, the accuracy is still met by this installation throughout the field of view, with some exceptions close to the Radar.

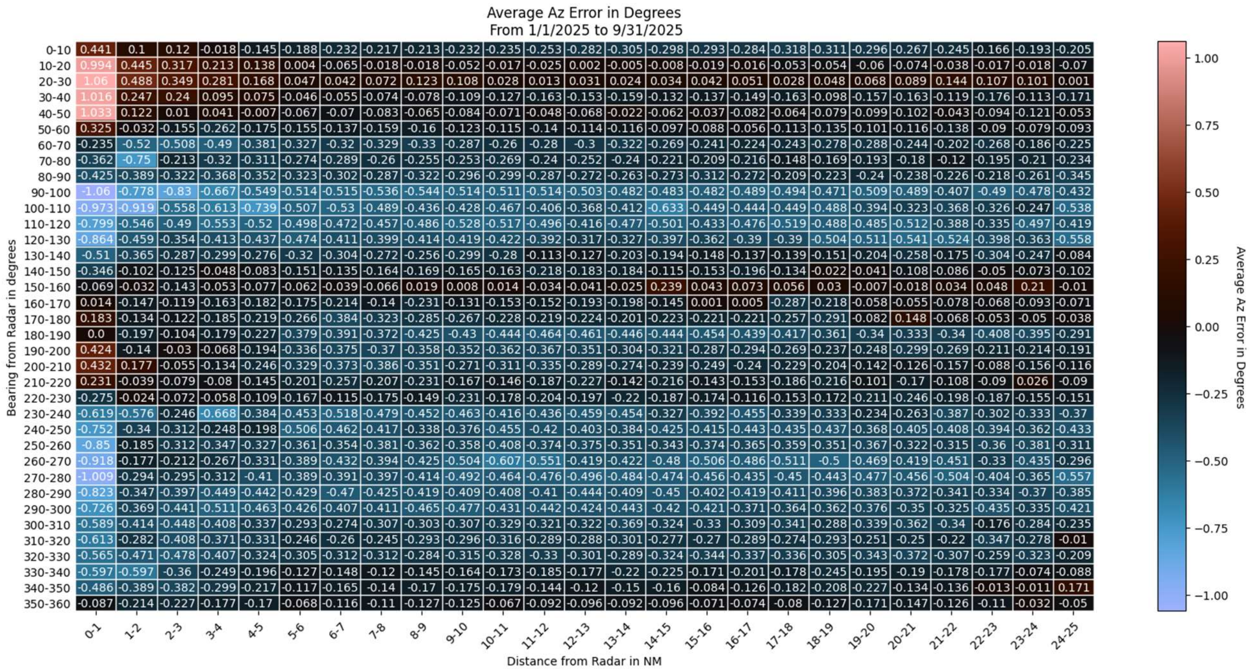

Figure 10: Average Azimuth Error of LSTAR

4.2.3 LSTAR Average Elevation

Figure 11 shows a heatmap based on the average elevation error between the correlated Radar and ADS-B tracks. Like the azimuth error, this value was pulled directly from the CSV files, summed based on each cell, and averaged based on the number of hits in that cell. Since the elevation error is calculated by subtracting ADS-B elevation from the Radar elevation, positive values result in Radar tracks that skew lower in altitude and negative values skew higher in altitude. The resulting heatmap shows a higher variance of results than the azimuth error. Since the instrumented elevation accuracy is 2.0 degrees for detections and 1.5 degrees for tracks, this is expected when compared to the azimuth. While most of the cells fall within the track error, there are multiple cells in the 130 degrees to 140 degrees bearing range around 9NM to 11NM outside that error. This range falls along the approach and departure path of ORF. There is also a large grouping of cells outside the range of 1.5 degrees around 210 degrees to 230 degrees bearing at 20NM or more. There are large errors within 1NM of the Radar similarly to the average azimuth and likely caused by the proximity to the sensor. Based on the values from the figure, many of the cells show positive values, indicating that the LSTAR typically skews low on altitude aside from within 1NM.

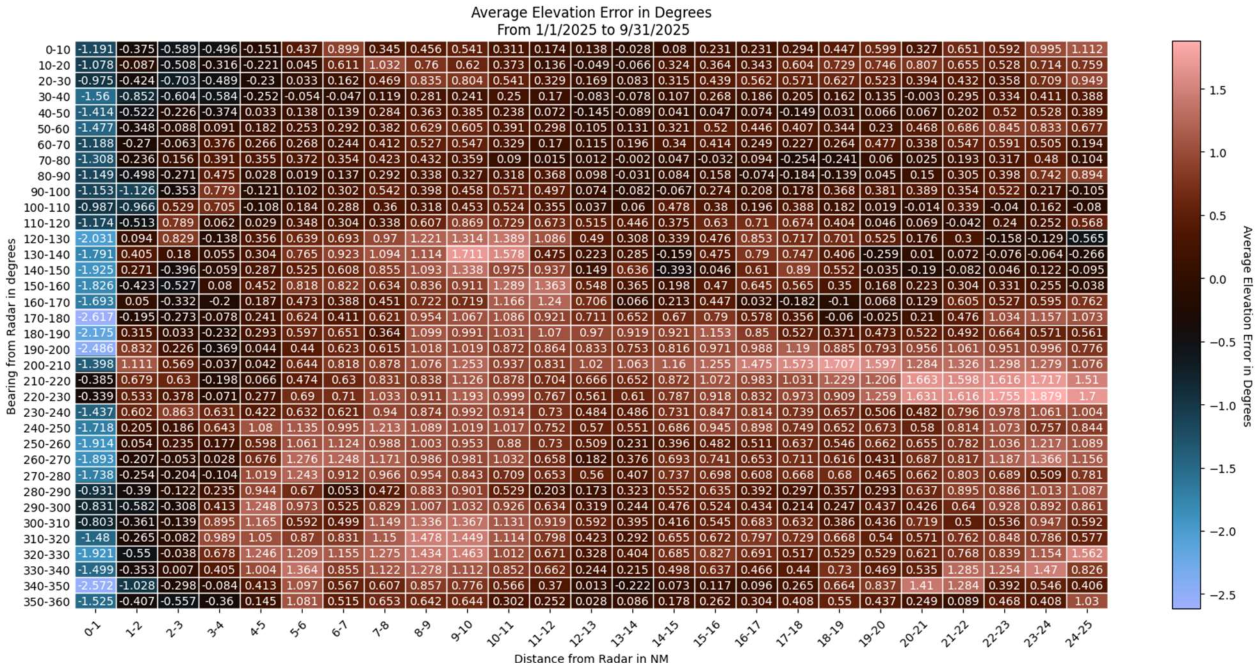

Figure 11: Average Elevation Error of LSTAR

4.2.4 LSTAR Average Range

Figure 12 shows a heatmap based on the average range error between the correlated Radar and ADS-B tracks. This value was calculated like the previous charts. Since the elevation error is calculated by subtracting ADS-B range from the Radar range, positive values result in Radar tracks that skew closer and negative values skew farther away. The resulting heatmap shows a couple of pockets of higher range errors, most notably at 18NM or more from the Radar and between 1NM to 2NM. The instrumented range accuracy for tracks is 25m, or roughly 0.0135NM, which increases to 30m for detections. There are numerous cells that fall outside this range, indicating large errors within range detection, however this is a much tighter accuracy specification than azimuth or elevation.

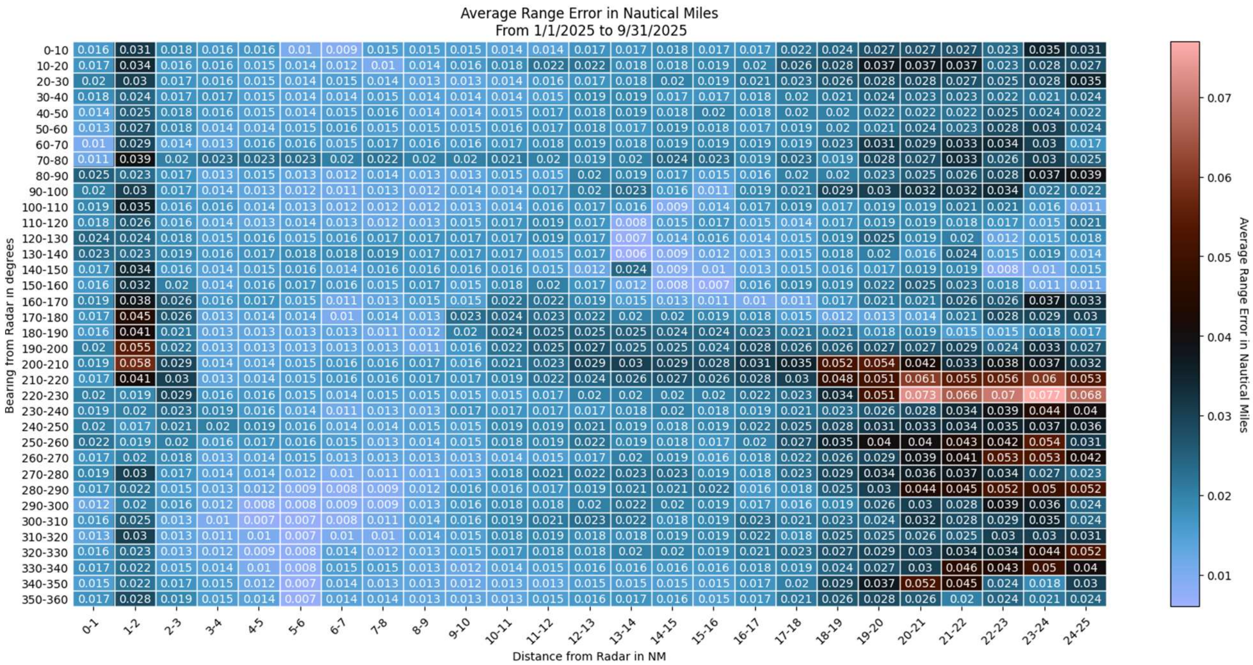

Figure 12: Average Range Errors of LSTAR

4.2.5 LSTAR Average Lateral Distance

Figure 13 shows a heatmap of the average lateral distances between correlated ADS-B and Radar tracks. This value was calculated using the haversine formula, which calculates the great-circle distance between two latitude and longitude points [9]. Each distance was summed and averaged based on the total hits in each cell to get the final value for a cell. Since this is lateral distance, this error is tied directly to the azimuth and range error. The effect of range error on this value is more consistent while the azimuth error will have a larger impact farther away from the sensor since a small amount of degree differences result in a larger lateral distance. This can be seen as the lateral distance increases as the target distance gets farther away from the Radar. For most of the coverage area, this lateral error is below 1000ft, however past 15NM, there is a higher likelihood of large errors of up 2000ft. Within 10NM, the lateral distance error is primarily below 500ft, providing fairly accurate estimates of position.

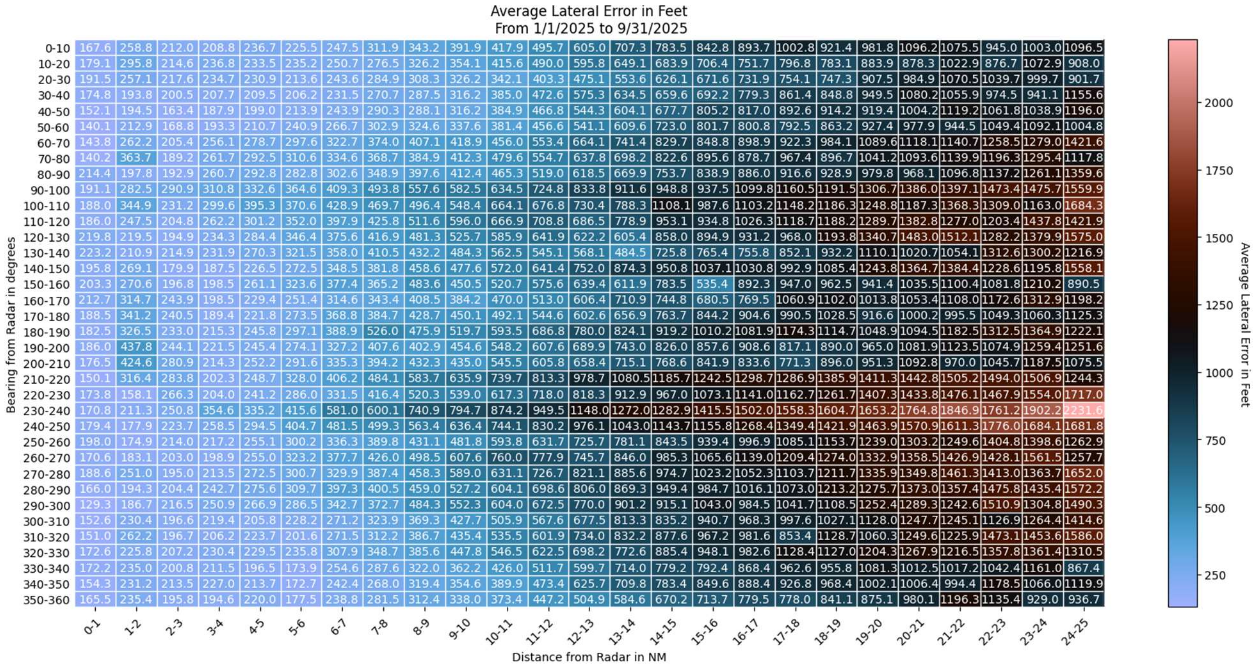

Figure 13: Average Lateral Error of LSTAR

4.2.6 LSTAR Average Altitude Distance

Figure 14 shows a heatmap of the average altitude error between correlated ADS-B and Radar tracks. This value was calculated by subtracting the ADS-B altitude from the Radar altitude of each track, summing the differences and averaging based on the total hits in each cell. The altitude error is tied directly to the elevation error, which has a similar effect as azimuth error on lateral distance as the range from the Radar increases. Positive values indicate that the ADS-B track reports its altitude higher than the Radar track and vice versa when negative. As the targets get farther away from the Radar, the altitude error goes from approximately +/- 200ft up to over +/- 4000ft in some spots, though those are mostly outside of the instrumented range of 40km, or 21.6NM. Aside from the 200 degrees to 230 degrees bearing, most of the average altitude errors within 21NM are within +/- 1500ft. There are many positive values, indicating that the LSTAR will typically project altitude lower than reality, but when within 4NM, more negative values are seen.

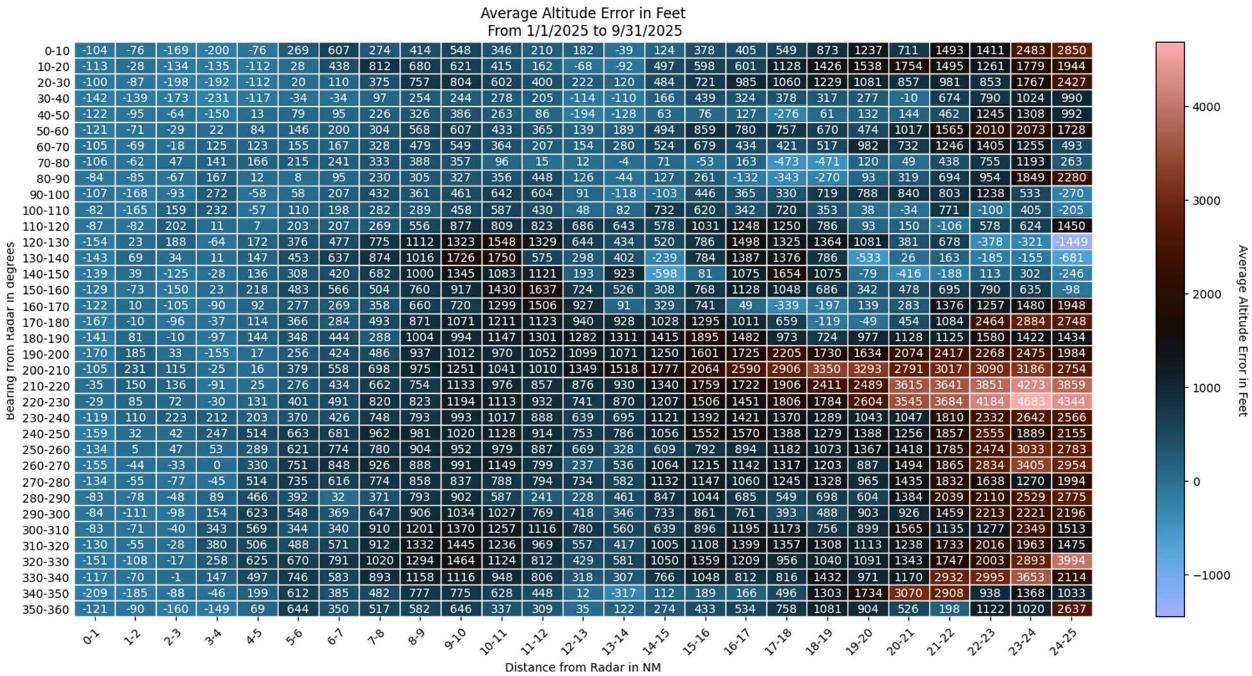

Figure 14: Average Altitude Error of LSTAR

4.2.7 LSTAR Altitude Skew

The percentage of Radar tracks with altitude under ADS-B tracks were calculated to explore how often the LSTAR Radar projects altitude below the ADS-B altitude. These percentages are calculated by summing the number of Radar hits below the correlated ADS-B altitude and divided by the total number of data points in each cell. Figure 15 shows a heatmap of these percentages in relation to their cells. Consistent with the altitude skew, most of the cells beyond 4NM are above 50% while the cells within are mostly below 50%. However, there are some cells, such as 130 degrees to 140 degrees bearing and 19NM to 20NM out, that have a negative average altitude but over 50% of the tracks skewed low, indicating that average altitude difference is not enough alone to determine skew in all cases.

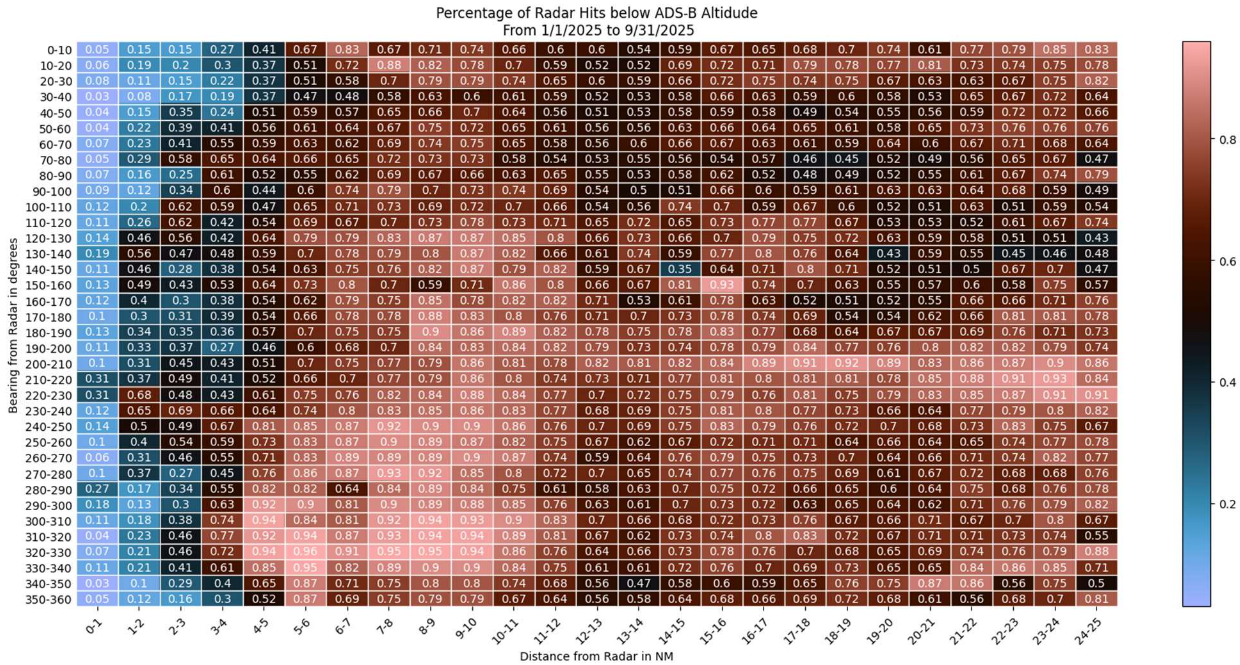

Figure 15: Percentage of Radar Hits below ADS-B Altitude of LSTAR

4.3 GA9120 Analysis

The GA9120 Radar only has roughly a 120 degrees field of view, an instrumented range of 15km (or 8.1NM) for large aircraft with a 12 degrees elevation angle, though that is adjustable up to 90 degrees [4]. For this data set, a 12 degrees elevation angle was used. Two GA9120 Radars were used for this data capture in the configuration discussed in Section 1.3 above. Like the LSTAR, values will be relative to the location of the Radar since the correlated data is based on that location. The same data matrix and ranges will be used. Based on the orientation of the Radars the expected azimuth coverage is expected to be from 0 degrees to 210 degrees. All calculations for the following sections are done in the same way as the LSTAR except they are done using the GA9120 correlated data for both Radars.

4.3.1 GA9120 Total Points

Figure 16 shows the total number of correlated hits picked up by both GA9120 Radars. Compared to the LSTAR, fewer targets are picked up, likely due to the reduced field of view of the GA9120 or lack of persistent tracking of a target for long enough to qualify a track for correlation. There are also very few tracks between 210 degrees to 360 degrees or past 9NM, which aligns with Radar orientation and specs. Many of the hits are around 7NM to 8NM away from the Radar between 130 degrees to 180 degrees bearing, which is located at the inlet of the James River into the Chesapeake Bay.

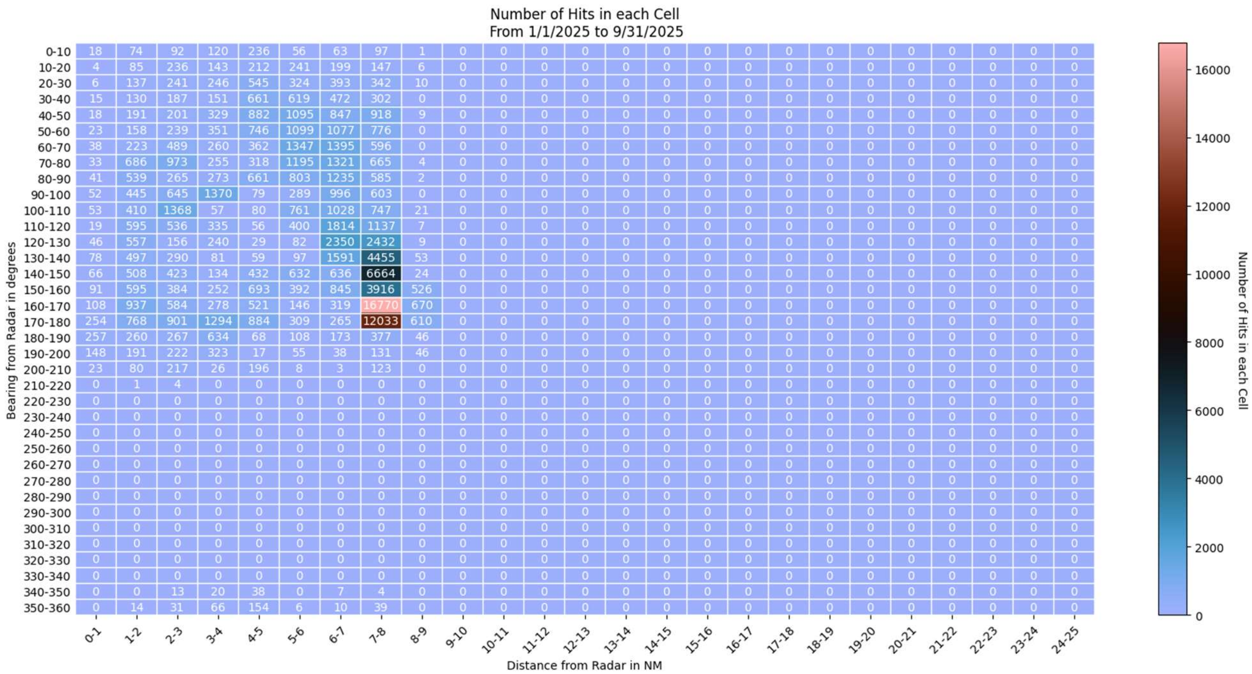

Figure 16: Total Number of Hits of GA9120s

4.3.2 GA9120 Average Azimuth

Figure 17 shows a heatmap of the average azimuth of the GA9120 Radars. The azimuth accuracy of this Radar is +/- 0.25 degrees according to the manufacturer specs. Many of the values in the results are within this range, however there are blocks that fall well outside of this range. Some only slightly fall outside of this range while others, mostly around the edge of the field of view, have a much larger error of over 1 degree. Since the ADS-B traffic is used as the bucketing criteria, this could be due to tracks that are retained for a short time when going outside of the field of view but are still correlated since correlation is over the lifetime of the track. The data filters remove a lot of this noise, but not all. This also does not explain the high error values in the middle of the field of view.

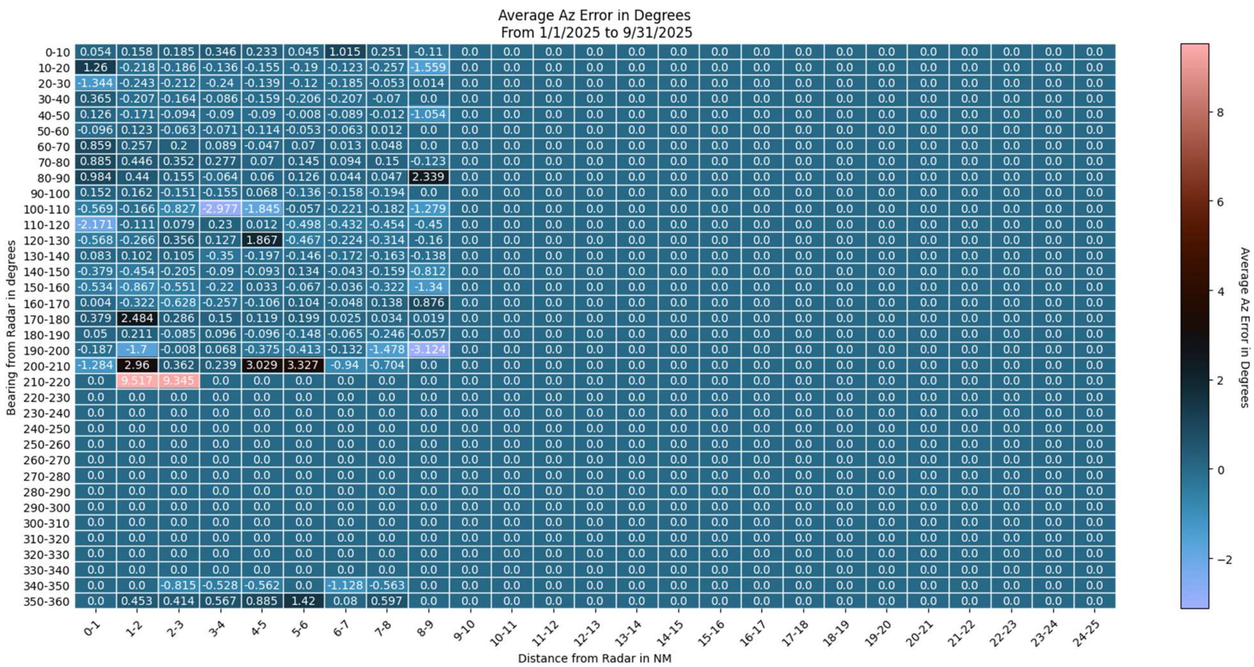

Figure 17: Average Azimuth Error of GA9120s

4.3.3 GA9120 Average Elevation

Figure 18 shows the average elevation errors of the GA9120 Radars. The elevation error of this Radar system varies from +/- 0.5 degrees up to +/- 2 degrees depending on the elevation field of view. Since the data is from GA9120s with a 12 degrees field of view, an accuracy of 0.5 will be assessed. The elevation error of the GA9120 covering 0 degrees to 120 degrees mostly hits this accuracy, however the south facing GA9120 generally falls outside of this range. This may be due to the 5-degree tilt on this sensor as opposed to the other sensor being level to the horizon. There are also large errors within 1NM of the sensors, likely due to higher sensitivity to elevation differences.

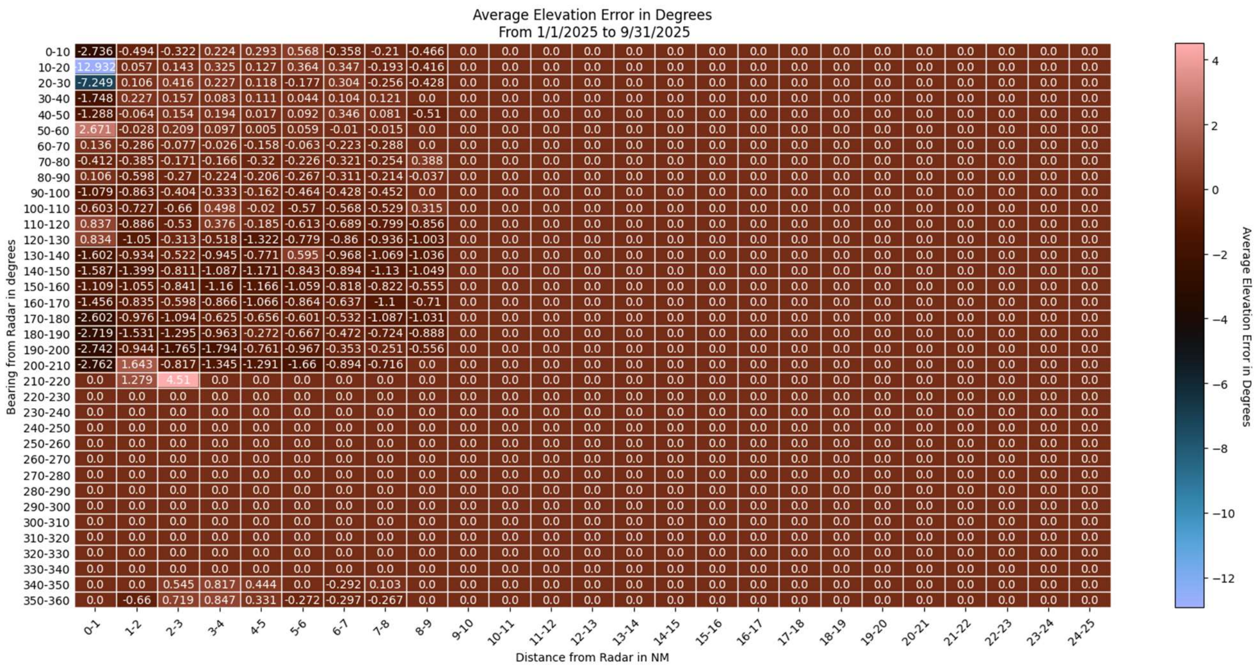

Figure 18: Average Elevation Error of GA9120s

4.3.4 GA9120 Average Range

Figure 19 shows the average range error for the GA9120s. The manufacture has no specifications on the range accuracy for this device, however, more values fall below 0.1NM with a handful of values on the edge of the field of view spiking higher.

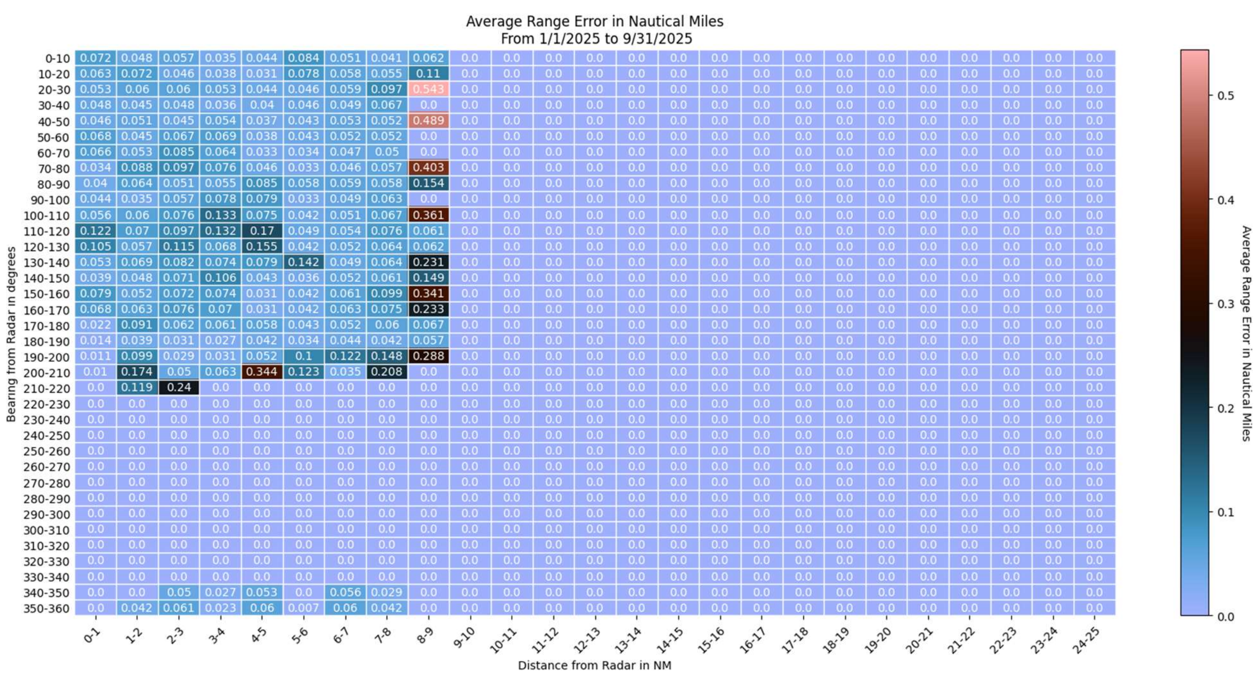

Figure 19: Average Range Error of GA9120s

4.3.5 GA9120 Average Lateral Distance

Figure 20 shows the average lateral error of the GA9120 systems. Unlike the LSTAR, there does not appear to be a large increase in error as targets get farther away from the Radars. There is a higher variance in the accuracy of the correlated tracks with average values going from below 100ft up to almost 2,500ft inside the field of view and large errors near the edge of the field of view.

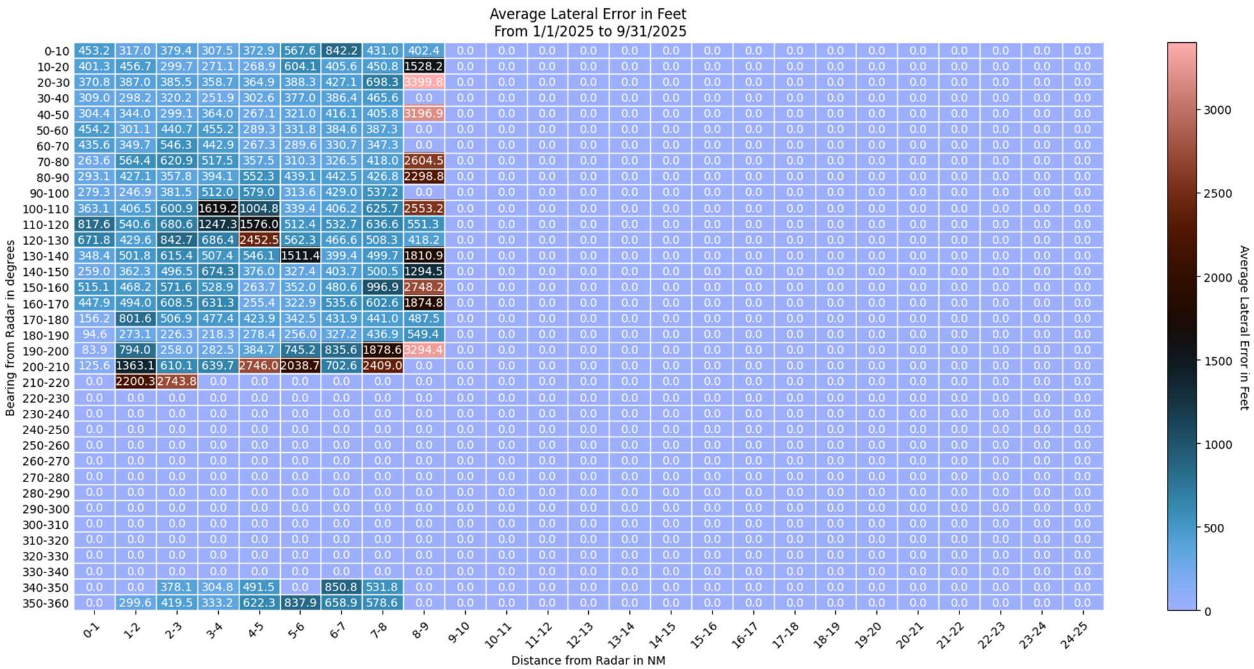

Figure 20: Average Lateral Error of GA9120s

4.3.6 GA9120 Average Altitude Distance

Figure 21 shows the average altitude errors of the GA9120 Radars. Altitude errors throughout mostly stay within 500ft with the errors growing higher on the south facing GA9120 as you get farther away from the sensor, up to almost 900ft. This is also seen on the other GA9120 but to a lesser extent, likely due to fewer tracks. Notably, most of the values are negative, indicating that the GA9120 is also reporting altitudes higher than the actual ADS-B altitude for the targets of opportunity.

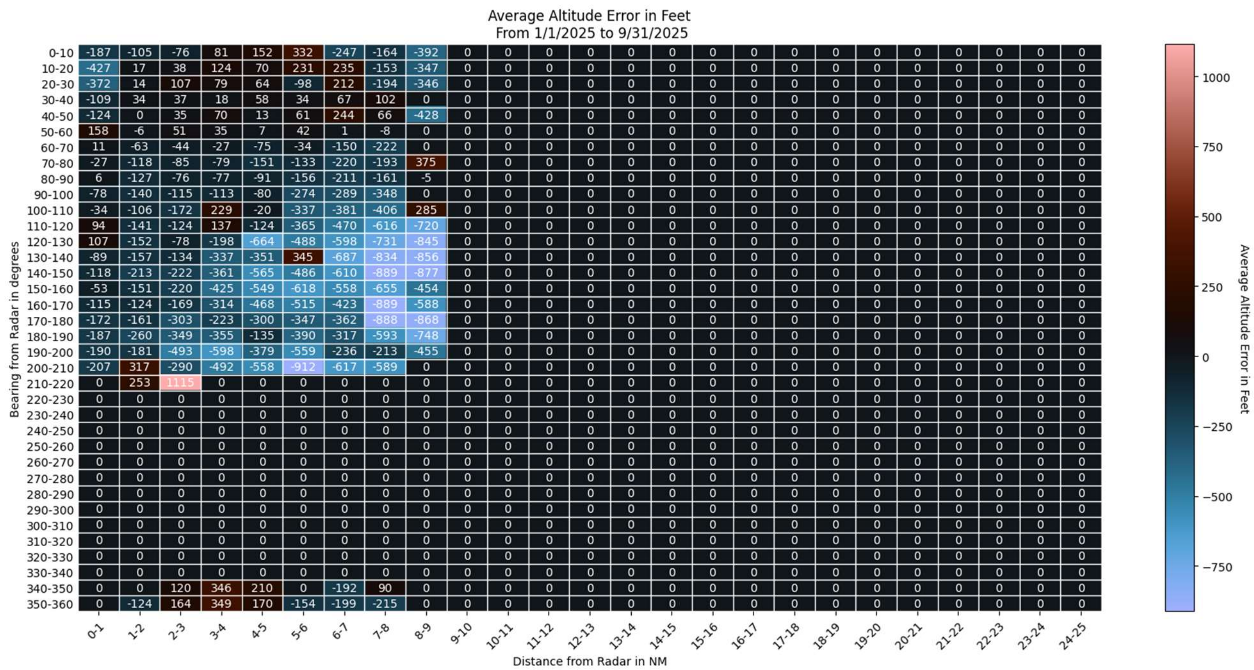

Figure 21: Average Altitude Error of GA9120s

4.3.7 GA9120 Altitude Skew

Figure 22 shows the percentage of Radar targets with altitude below their correlated ADS-B target. This confirms that most of the tracks are skewed low from the GA9120 facing the south while the other GA9120 is more balanced. Interestingly, the cells with the highest number of hits still have a very low percentage of hits above the ADS-B track, indicating that this is a consistent occurrence.

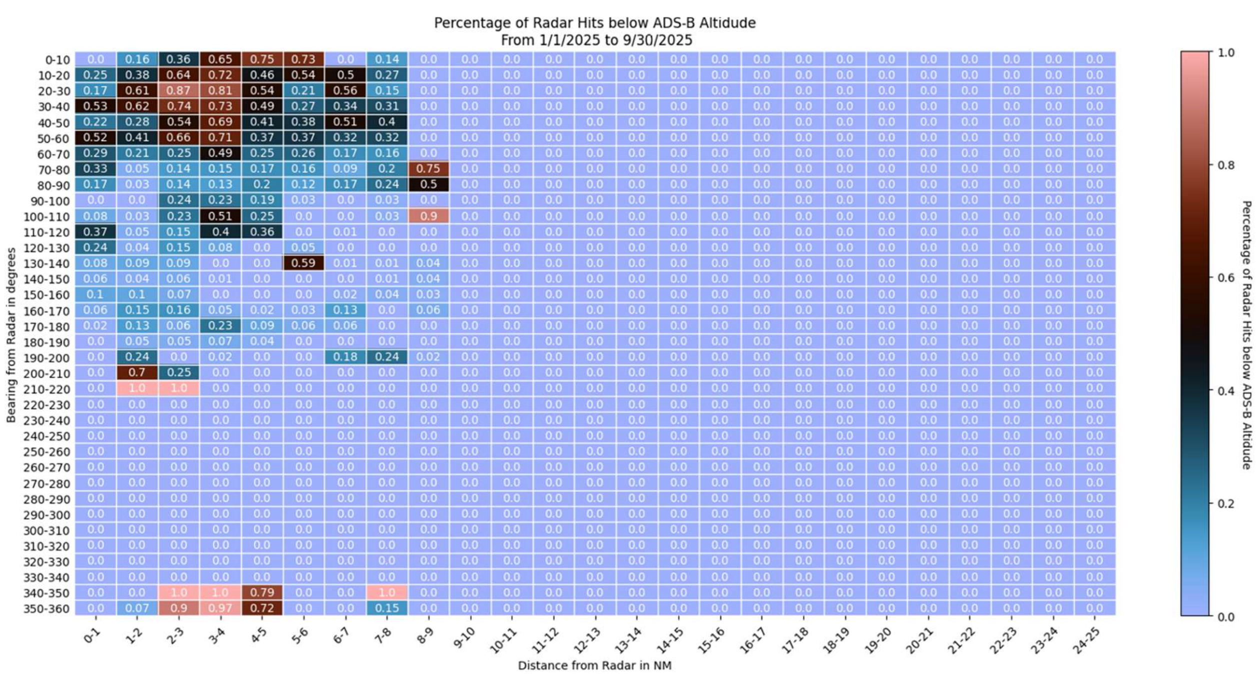

Figure 22: Percentage of Radar Hits Below ADS-B Altitude of GA9120s

5.0 Conclusions

The data pulled over the 9-month period between January 1st, 2025 and September 30th, 2025 give us a long-term view of the performance of the Radar on a variety of different targets. During this period, 4,678,668 valid correlated points were used for the LSTAR data outputs after filters were applied, and 116,647 points were used for both GA-9120 Radars in the combined output. While target type is not specifically examined in this report, it is desired to have diversity in targets to determine how well the Radars perform in a diverse airspace. It is important to note that only aircraft emitting an ADS-B signal were considered. Since NASA Langley Research Center is located near Langley Air Force Base and other military bases in the Hampton Roads Area, there were likely aircraft picked up by the Radar without an ADS-B emitter on, so this is not a comprehensive view of all targets picked up by the Radar.

5.1 LSTAR Conclusions

When comparing the LSTAR results to the manufacturer specifications, the Radar generally falls within specifications for azimuth and elevation error, occasionally exceeds the instrumented range, but typically falls outside of the range accuracy metric, especially past 10NM. Even though the elevation and azimuth tend to fall within specifications, within 1NM of the Radar tends to yield high errors well outside of the specification. This is likely due to lateral errors adding larger differences to elevation and azimuth errors when this close to the Radar. Since the number of aircraft within this area is very low compared to the rest of the cells, this is not believed to be a significant hinderance. The altitude and lateral distance show how large the errors become as you move away from the Radar, even when elevation and azimuth errors are within specification. Laterally, the Radar tends to be accurate to within 500ft up to 10NM. Past 10NM the lateral accuracy becomes larger than 500ft, getting worse as the distance increases. A similar trend can be seen with altitude differences increasing as the track gets farther from the Radar, but there are pockets of higher accuracy values throughout. This may be due to averaging errors of positive and negative values. When looking at the frequency of Radar track's altitude being lower than ADS-B reported altitude, most cells beyond 5NM show more than 50% of the tracks having a lower altitude than the ADS-B, but within 4NM shows that it's more likely for a track to have a higher altitude than the ADS-B track. The total hits graph shows two major hot spots, one at 13NM and 120 degrees bearing and another at 5NM and 300 degrees bearing. The first hotspot is the airport located in Norfolk, Virginia and the second hotspot is the airport in Newport News, Virginia, which can be seen in Figure 23. The remaining circle plots for the LSTAR can be seen in Appendix A: LSTAR Circle Plots.

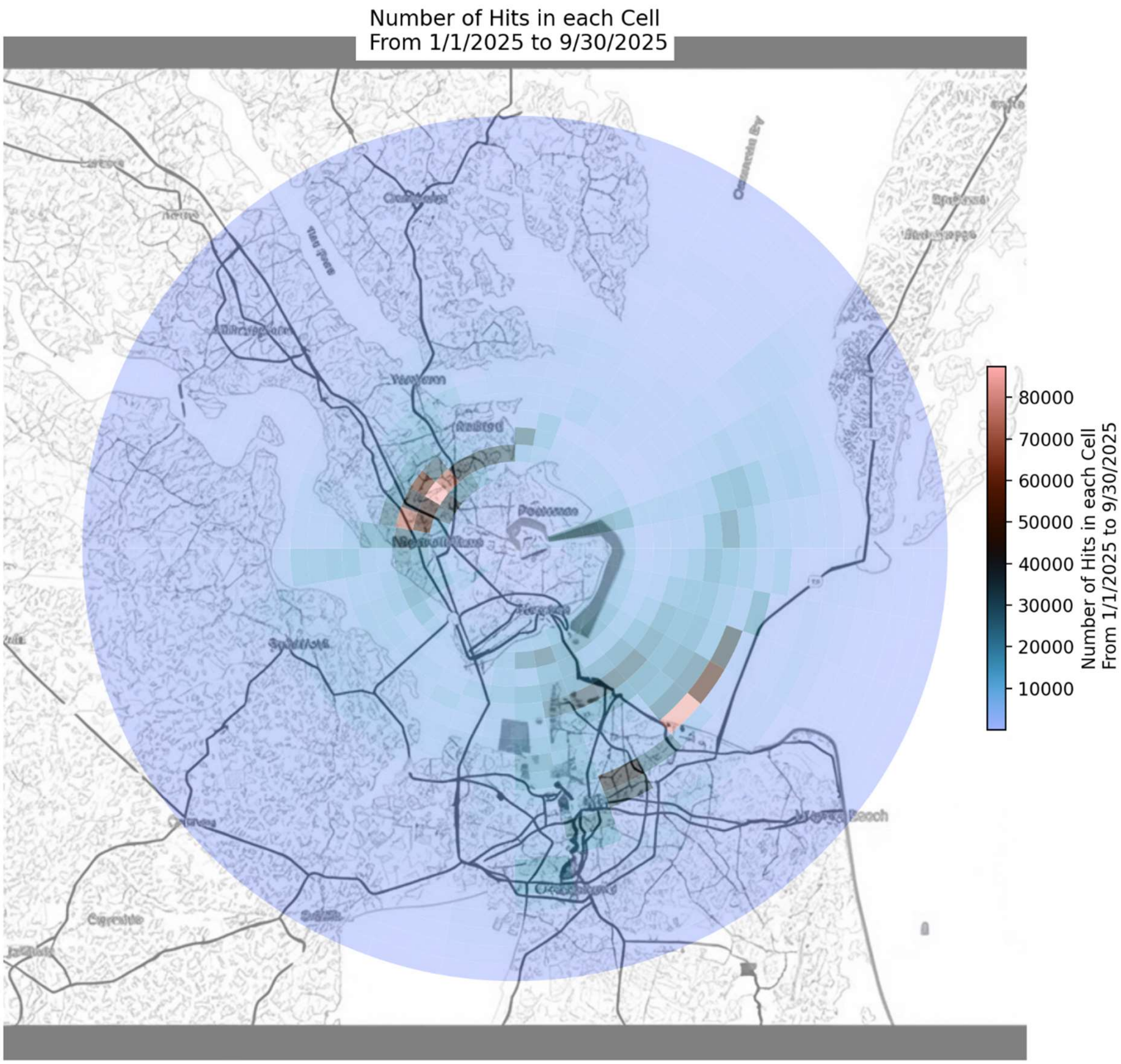

Figure 23: Circler Plot of Hits from the LSTAR

5.2 GA-9120 Conclusions

When looking at the outputs of the GA-9120, the effective range is between 8NM and 9NM with most of the hits coming between 7NM and 8NM. This seems to be in line with the instrumented range of 15km, or roughly 8.1NM. The azimuth of both Radars also covers from 340 bearing to 210 bearing, which is around 230 degrees of view, in line with the 120 degrees field of view per Radar. When looking at azimuth errors, the specifications state that an error of 0.25 degrees is expected. While some cells within the field of view meet this accuracy, most of the cells seem to fall outside of it, with errors up to three degrees near the edge of the sensor’s field of view. A similar trend can be seen with the elevation as well, which is expected to have an accuracy of 0.5 degrees. While some cells fall within this range, particularly for the Radar that covers the 340 degrees to 360 degrees and 0 degrees to 100 degrees range, there are still many cells that fall outside of this range. The effects of azimuth and elevation error can be seen within the lateral and altitude error plots, respectively. As expected, the higher the azimuth or elevation error, the larger the distance errors are. Compared to the LSTAR, the GA-9120 Radars allow for more Radar configuration, which may improve the accuracy metrics for large aircraft. Circle Plots for the GA9120s that can be seen in Appendix B: GA9120 Circle Plots.

6.0 Suggestions for Future Work

The scripts discussed in this TM lay out the groundwork for the analysis of the Radar systems currently available to researchers at NASA Langley Research Center. For future consideration, the authors believe it would be useful to divide the Radar coverage area into equal segments and to then analytically determine the effectiveness of each Radar system inside of each segment, using the latitude error, longitude error and altitude error in that segment. In this manner the user could compare the effectiveness of each Radar system in each segment and therefore make recommendations as to which Radar unit or combination of units would be the most appropriate for use in each segment of the coverage area. This would assist future flight operations in determining which Radar system would best support the needs of that specific (future) flight.

Additional analysis should be performed on the presented data, such as looking at each point individually to determine if it is within the manufacturer specifications for azimuth, elevation and range. These points can then be summed up and displayed in a similar fashion to the figures in the analysis section, both as totals and as percentages of points. The standard deviation of the data sets presented in this report should also be calculated to observe the variance of the data presented to understand how close these averages represent the data coming in. The team could further evaluate performance by determining aircraft type from the ADS-B data and determine detection performance based on aircraft type. Finally, further investigation into the configuration of the radar systems to further tune radars for performance could be conducted, specifically on the GA9120s as the LSTAR configuration is more limited. This would require another period of data collection, either through targets of opportunity or through coordinated test flights.

References

[1] M. W. Coldsnow, L. J. Glaab, J. Revesz, L. O. Kagey, R. G. McSwain and J. R. Schaefer, "Safety Case for Small Uncrewed Aircraft Systems (sUAS) Beyond Visual Line of Sight (BVLOS) Operations at NASA Langley Research Center Research Center," NASA/TM–20230003007, Hampton, VA, 2023.

[2] J. T. Revesz, J. T. Unverricht, B. J. Petty, B. K. Buck and L. J. Glaab, "Advancements in Remote Ground Control Station Operator Pilot in Command Training Program for Beyond

Visual Line of Sight Flight Operations," in *American Institute of Aeronautics and Astronautics Aviation*, Las Vegas, NV, 2024.

[3] SRC Inc., "OPERATOR GUIDE FOR Radar SET LSTAR (V)2," 2015.

[4] Observation Without Limits (OWL), March 2021. [Online]. Available: https://owlknows.com/wp-content/uploads/2021/06/OWL_GA9120_AE-Spec_3-26-21.pdf. [Accessed 23 12 2025].

[5] Colins Aerospace, "Skyler," 2025. [Online]. Available: https://www.rtx.com/collinsaerospace/what-we-do/industries/air-traffic-management/surveillance/skyler. [Accessed 2025].

[6] FLARM Technology AG, "About us: FLARM," FLARM Technology AG, [Online]. Available: https://www.flarm.com/en/about-us/.

[7] EUROCONTROL, "All-purpose structured EUROCONTROL surveillance information exchange," 22 October 2025. [Online]. Available: https://www.eurocontrol.int/asterix. [Accessed 2025].

[8] NASA, "CSS Archive," 1 April 2022. [Online]. Available: https://css-www.larc.nasa.gov/archive/?doing_wp_cron=1766073251.5276679992675781250000. [Accessed 2025].

[9] Movable Type Scripts, "Calculate distance, bearing and more between Latitude/Longitude points," [Online]. Available: https://www.movable-type.co.uk/scripts/latlong.html. [Accessed 23 12 2025].

Appendix A: LSTAR Circle Plots

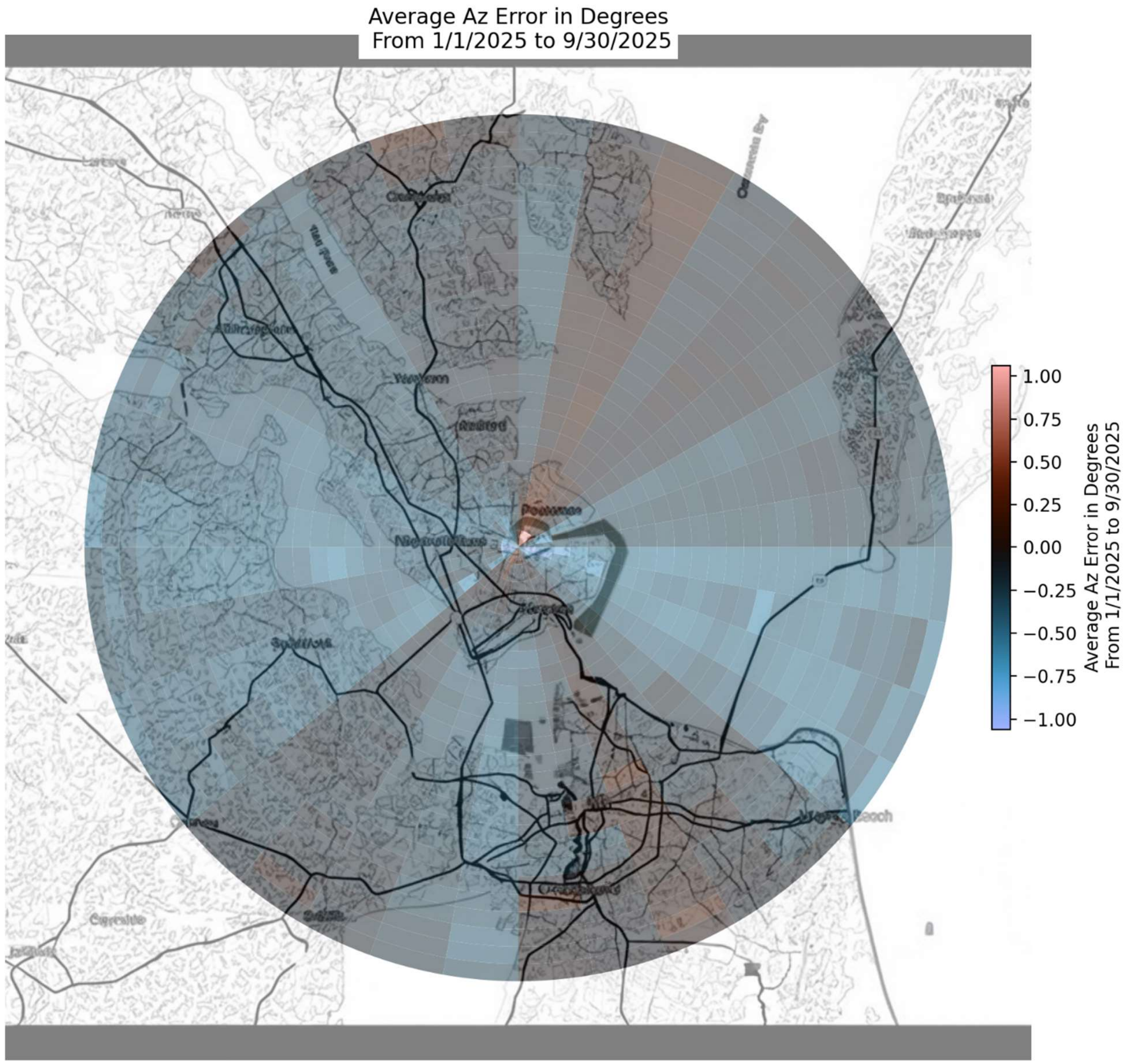

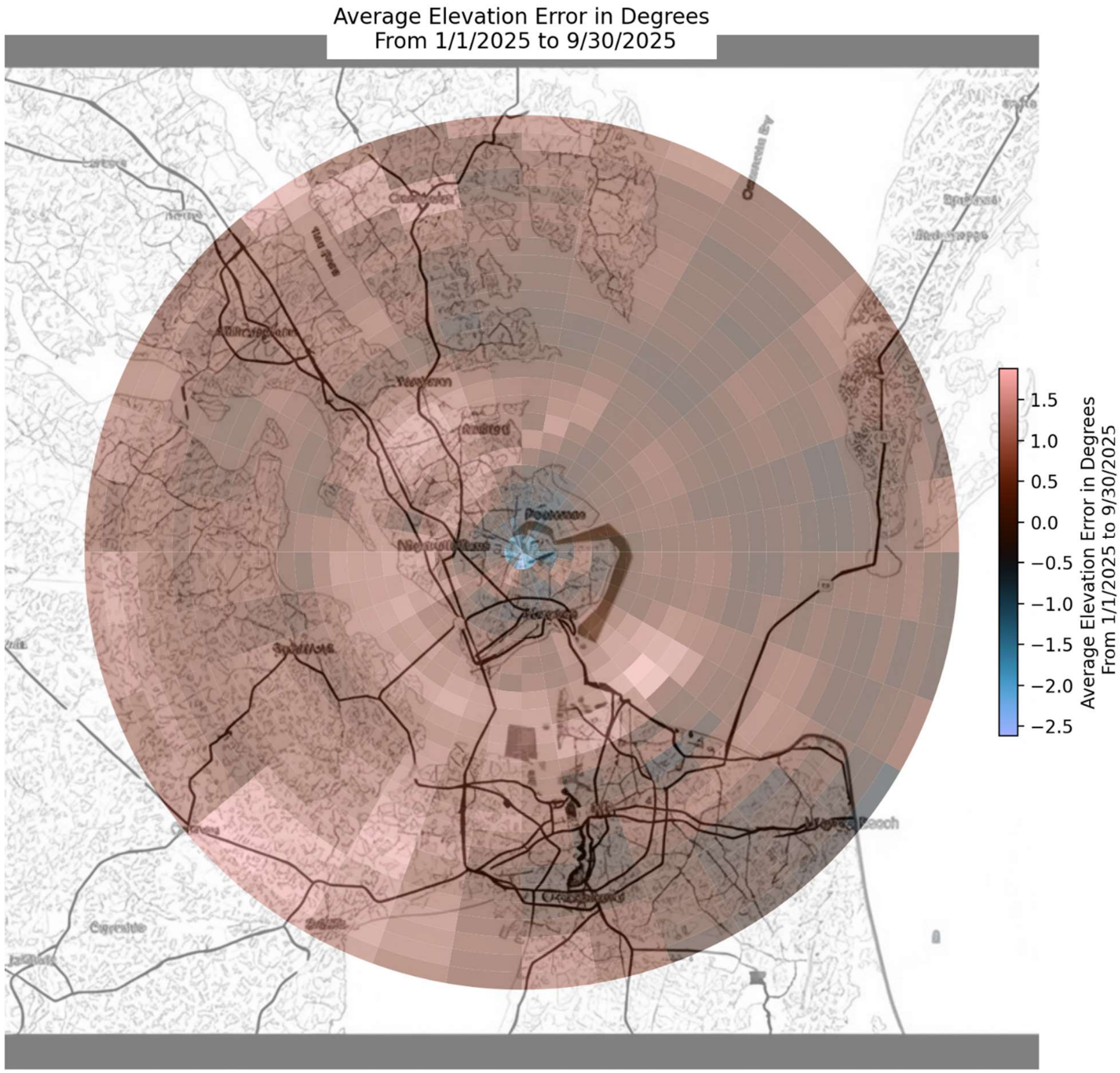
Average Elevation Error in Degrees
From 1/1/2025 to 9/30/2025
1.5
1.0
0.5
0.0
−0.5
−1.0
−1.5
−2.0
−2.5
Average Elevation Error in Degrees
From 1/1/2025 to 9/30/2025

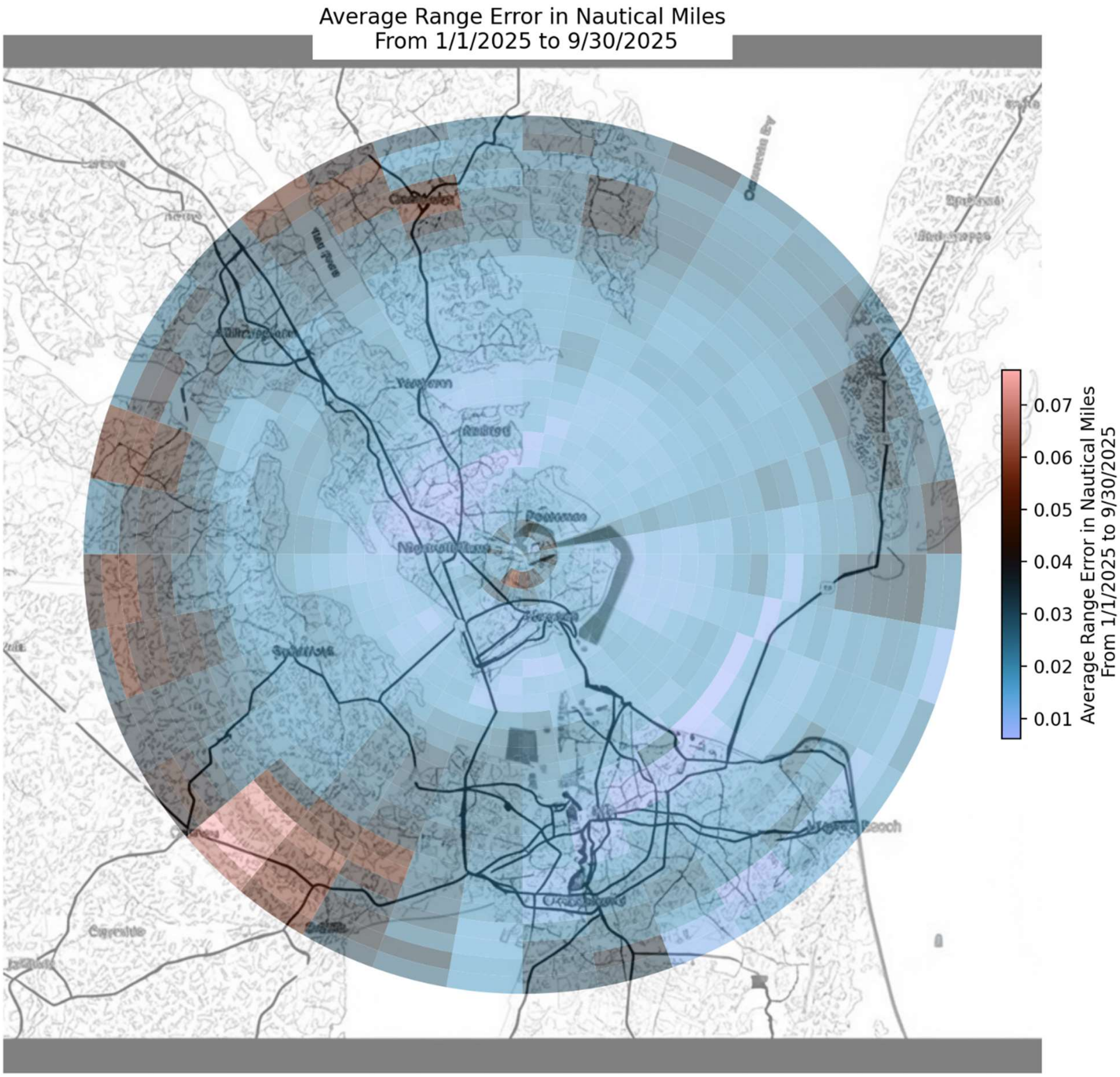
Average Range Error in Nautical Miles
From 1/1/2025 to 9/30/2025
Average Range Error in Nautical Miles
From 1/1/2025 to 9/30/2025
0.07
0.06
0.05
0.04
0.03
0.02
0.01

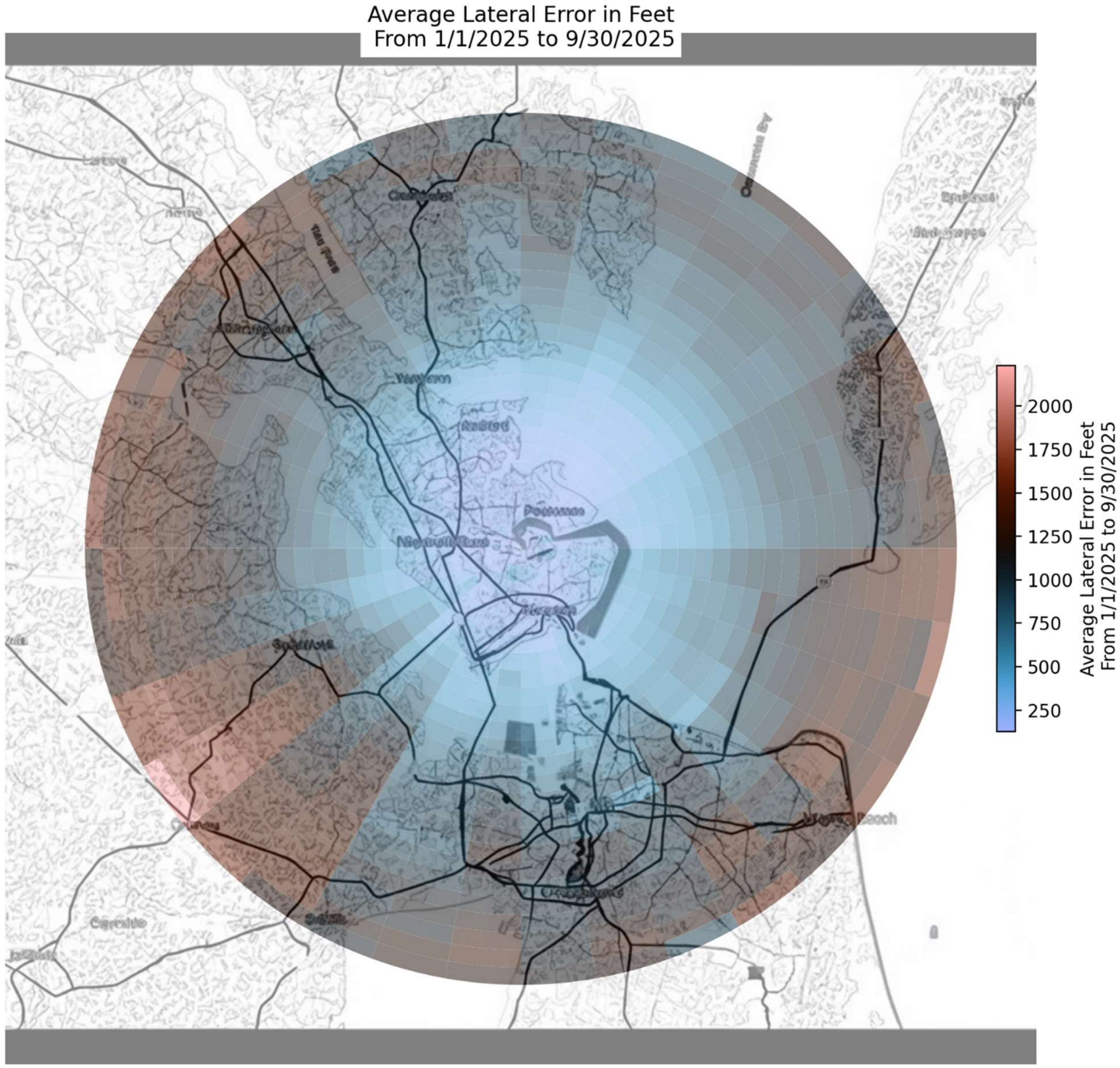
Average Lateral Error in Feet
From 1/1/2025 to 9/30/2025
2000
1750
1500
1250
1000
750
500
250
Average Lateral Error in Feet
From 1/1/2025 to 9/30/2025

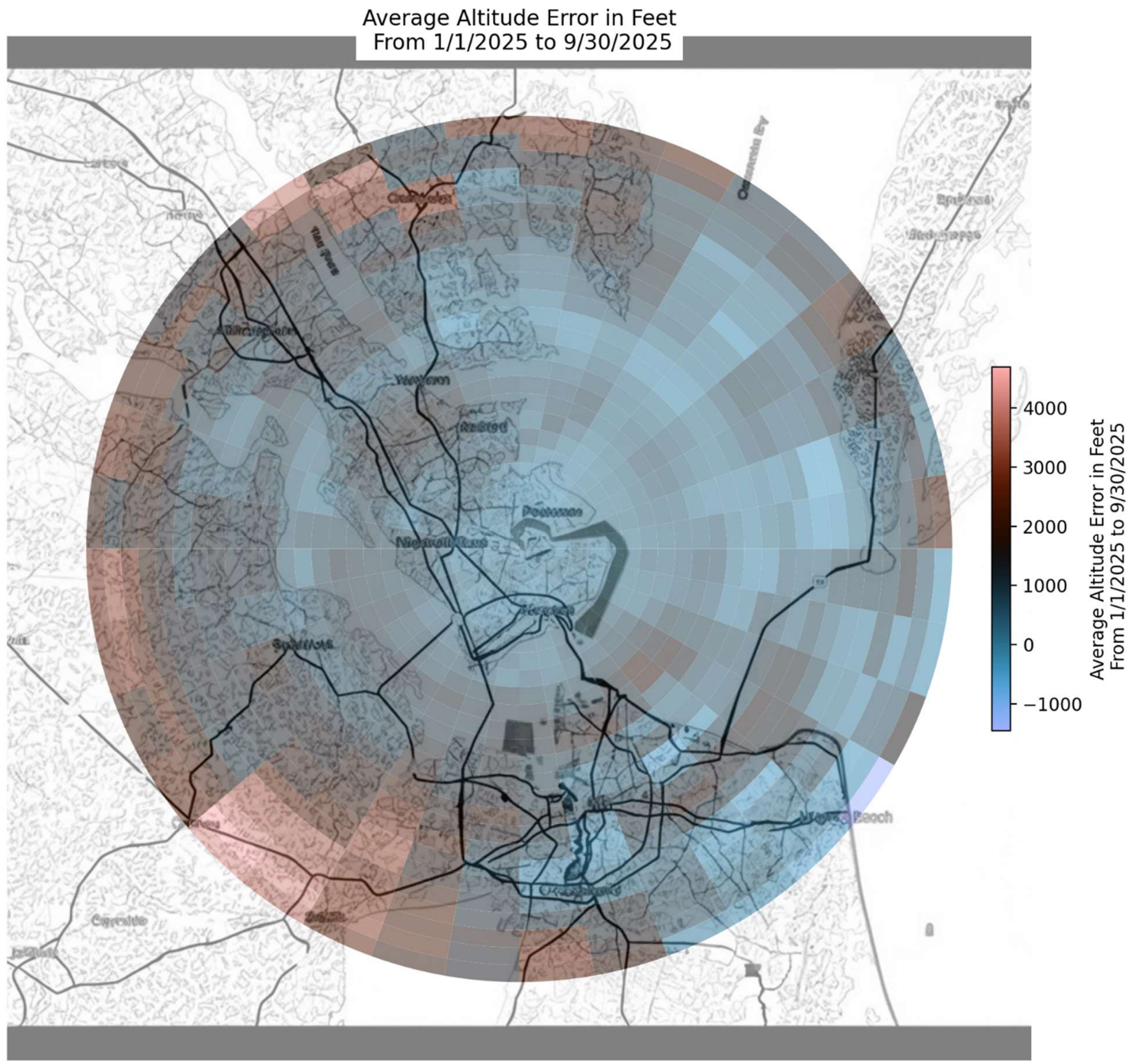
Average Altitude Error in Feet
From 1/1/2025 to 9/30/2025
4000
3000
2000
1000
0
−1000
Average Altitude Error in Feet
From 1/1/2025 to 9/30/2025

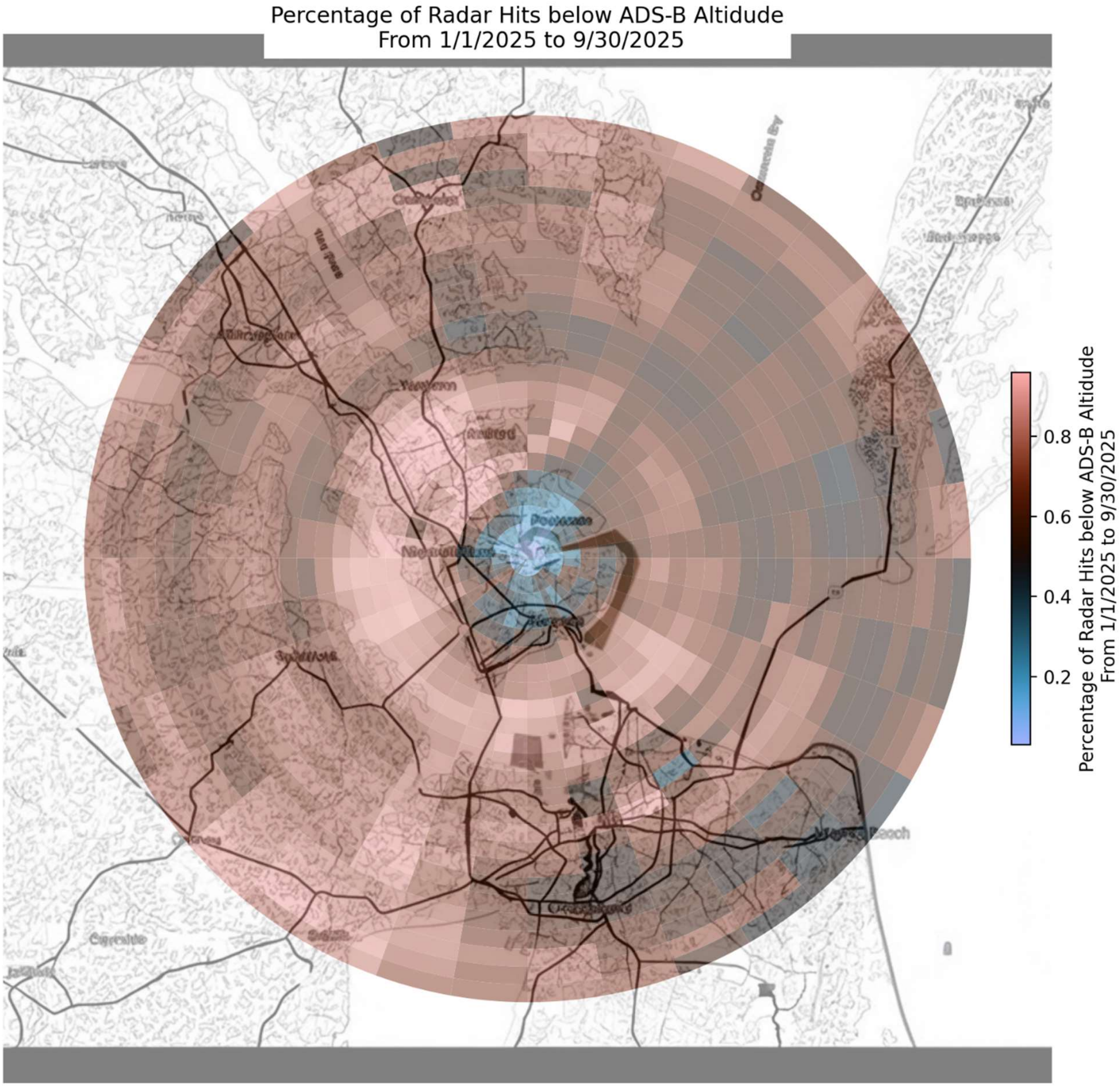
Percentage of Radar Hits below ADS-B Altidude
From 1/1/2025 to 9/30/2025
0.8
0.6
0.4
0.2
Percentage of Radar Hits below ADS-B Altidude
From 1/1/2025 to 9/30/2025

Appendix B: GA9120 Circle Plots

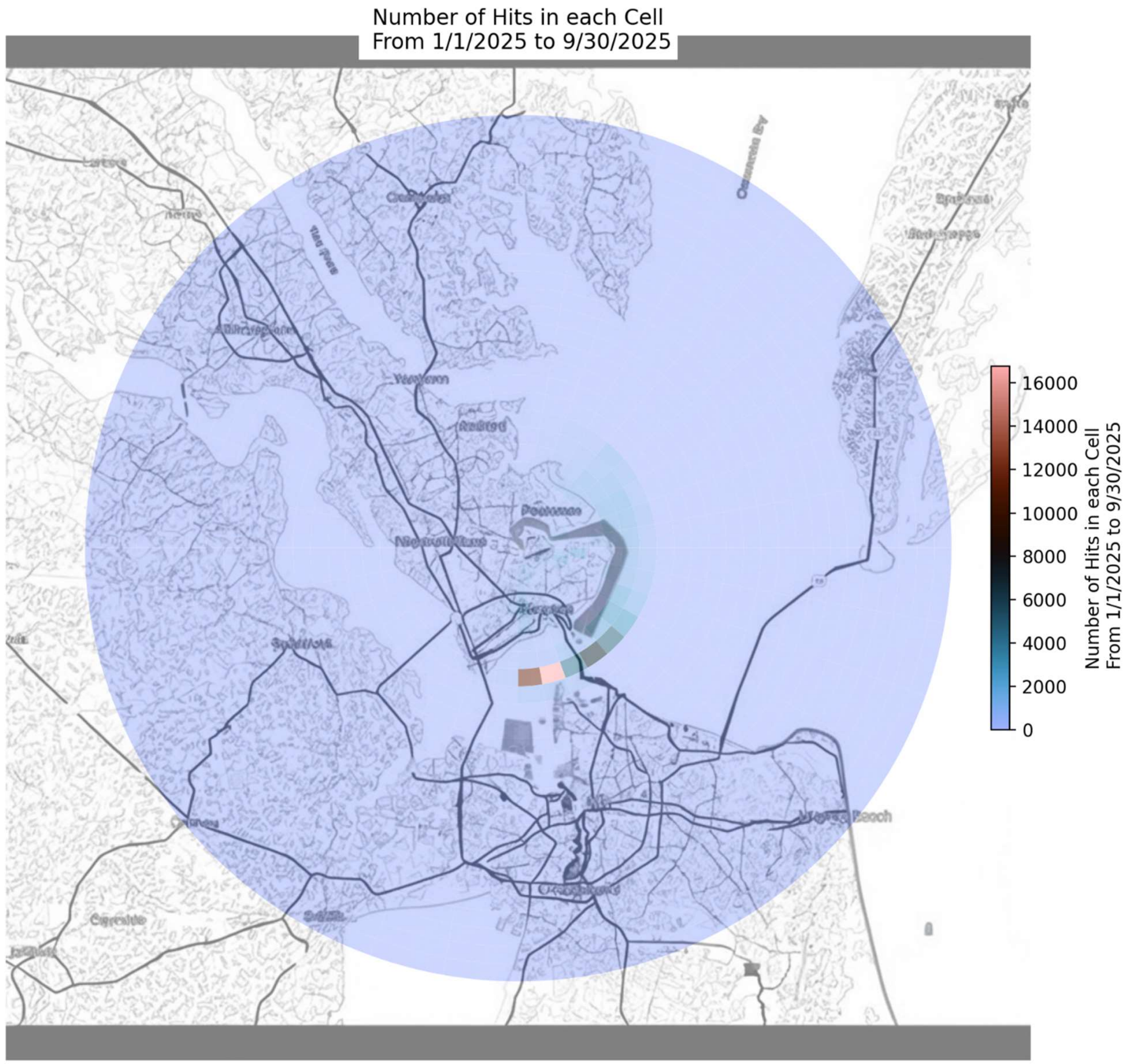

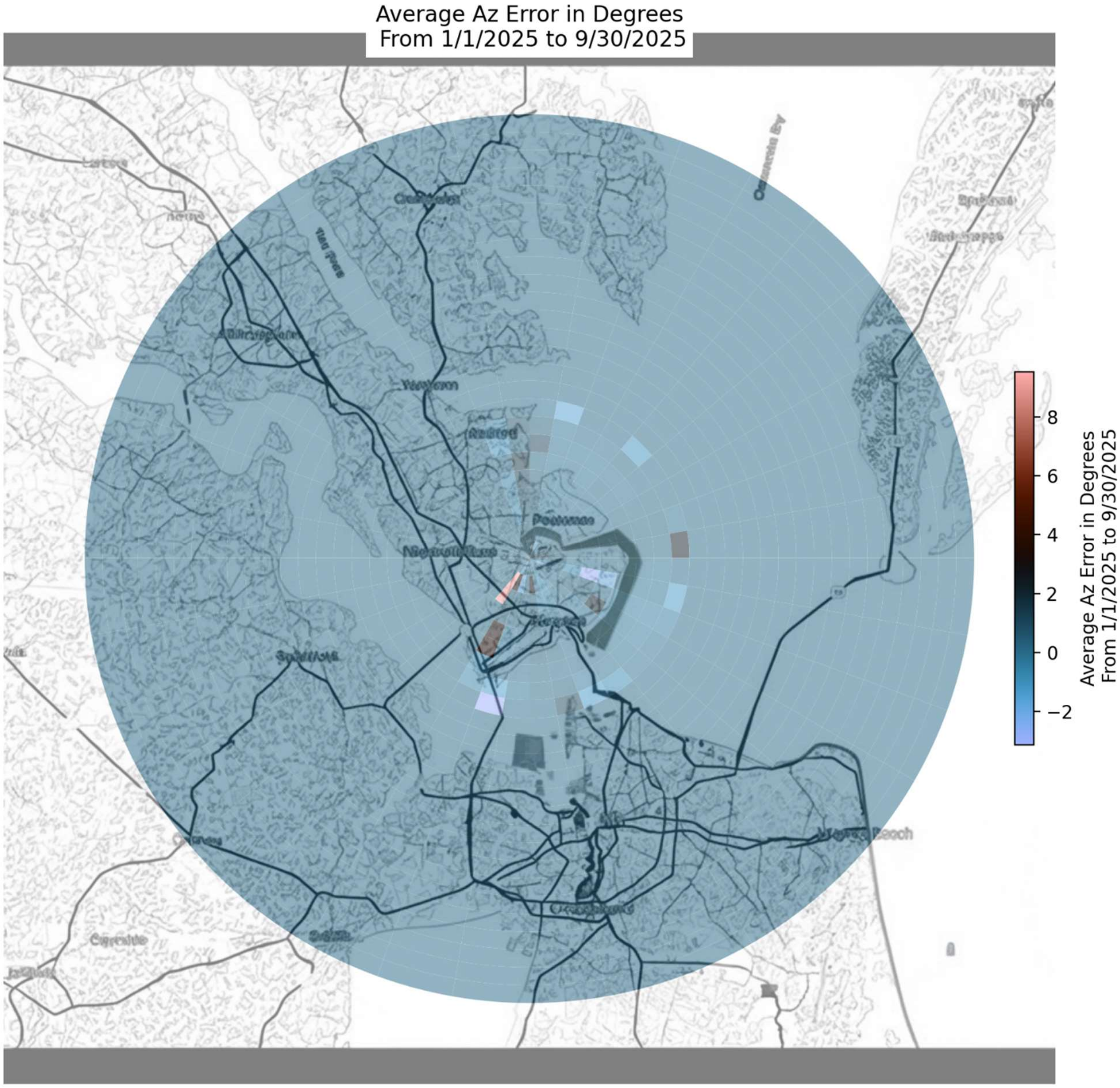
Average Az Error in Degrees
From 1/1/2025 to 9/30/2025
8
6
4
2
0
−2
Average Az Error in Degrees
From 1/1/2025 to 9/30/2025

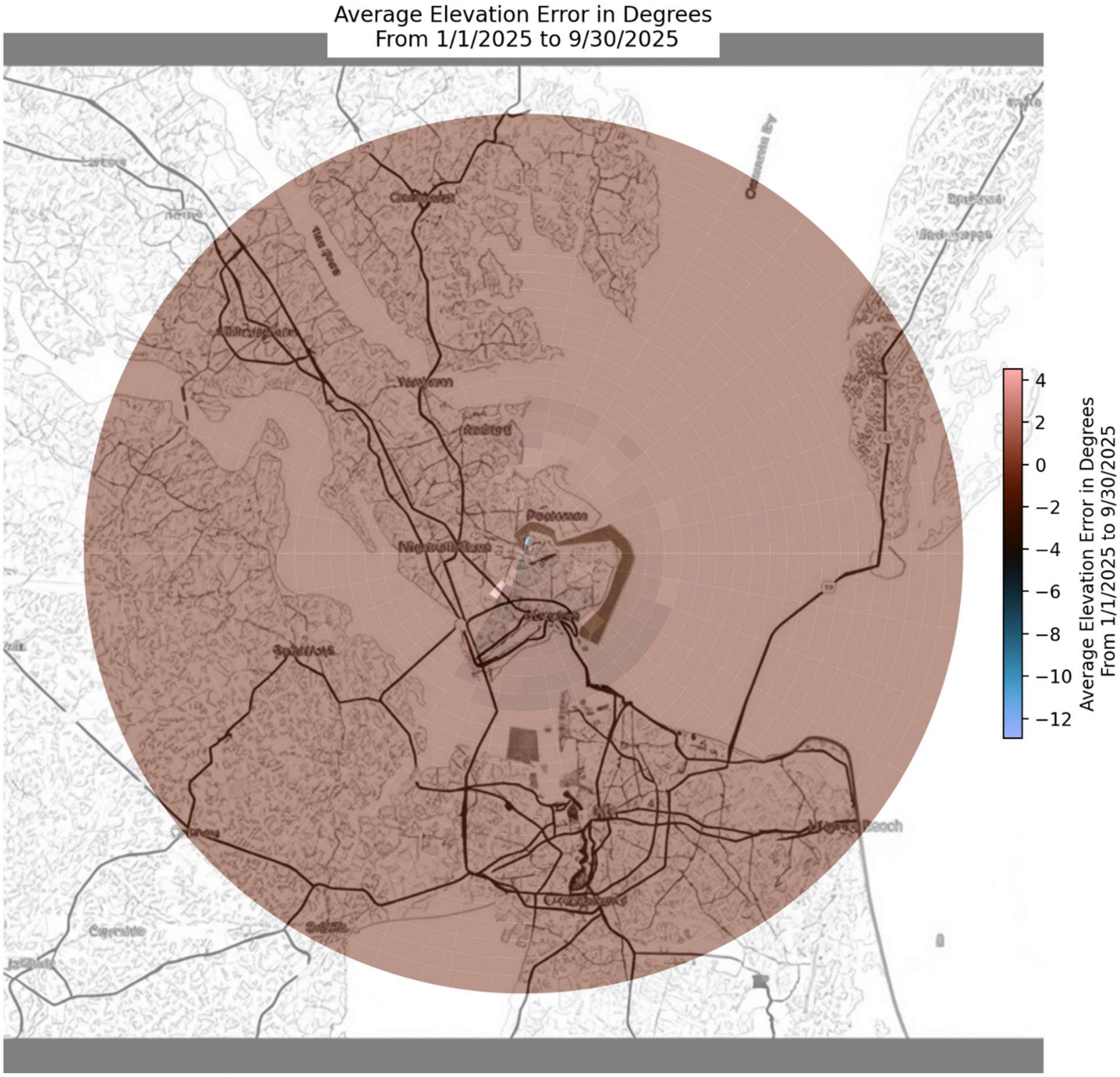
Average Elevation Error in Degrees
From 1/1/2025 to 9/30/2025
4
2
0
−2
−4
−6
−8
−10
−12
Average Elevation Error in Degrees
From 1/1/2025 to 9/30/2025

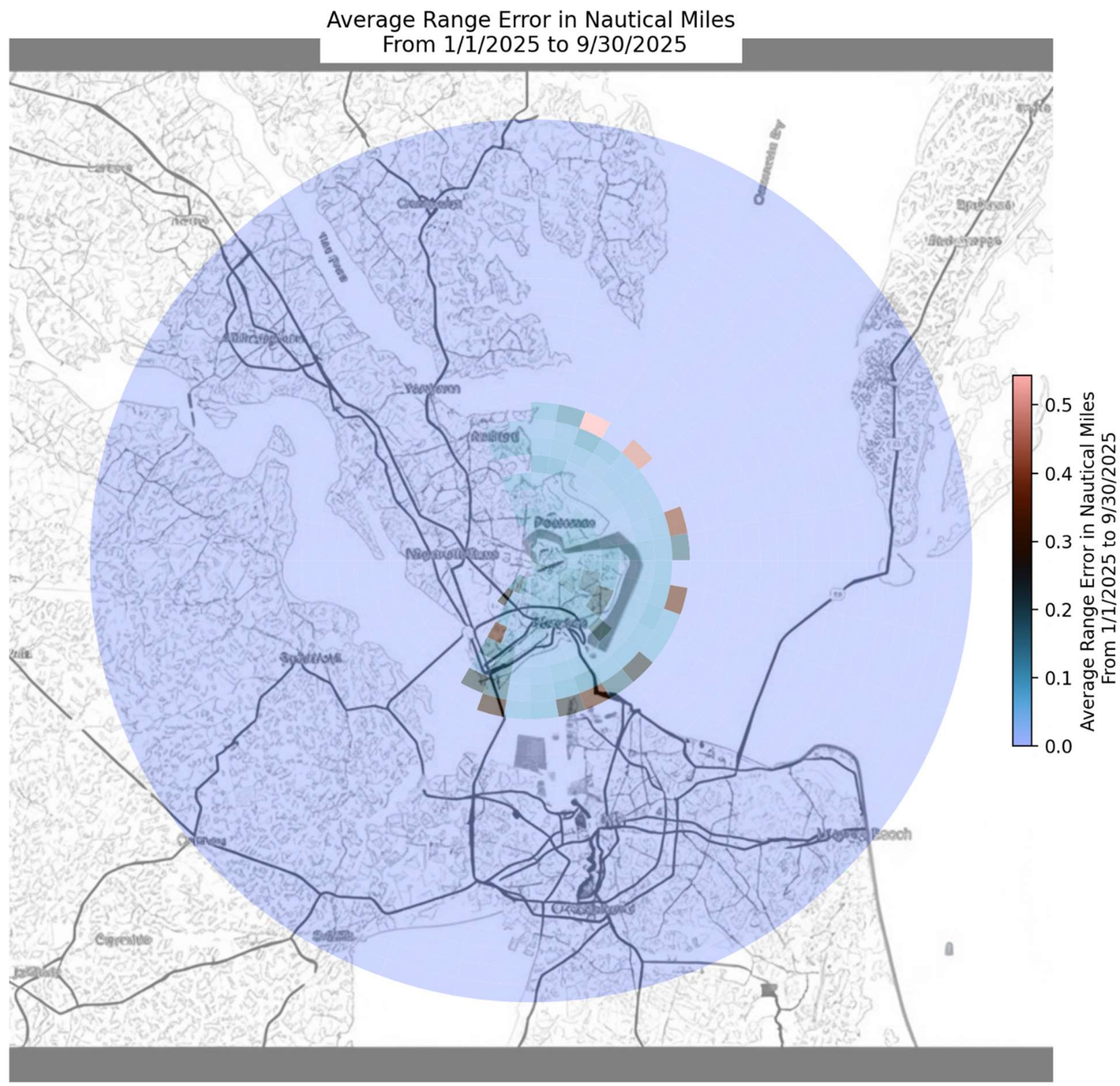
Average Range Error in Nautical Miles
From 1/1/2025 to 9/30/2025
Average Range Error in Nautical Miles
From 1/1/2025 to 9/30/2025
0.5
0.4
0.3
0.2
0.1
0.0

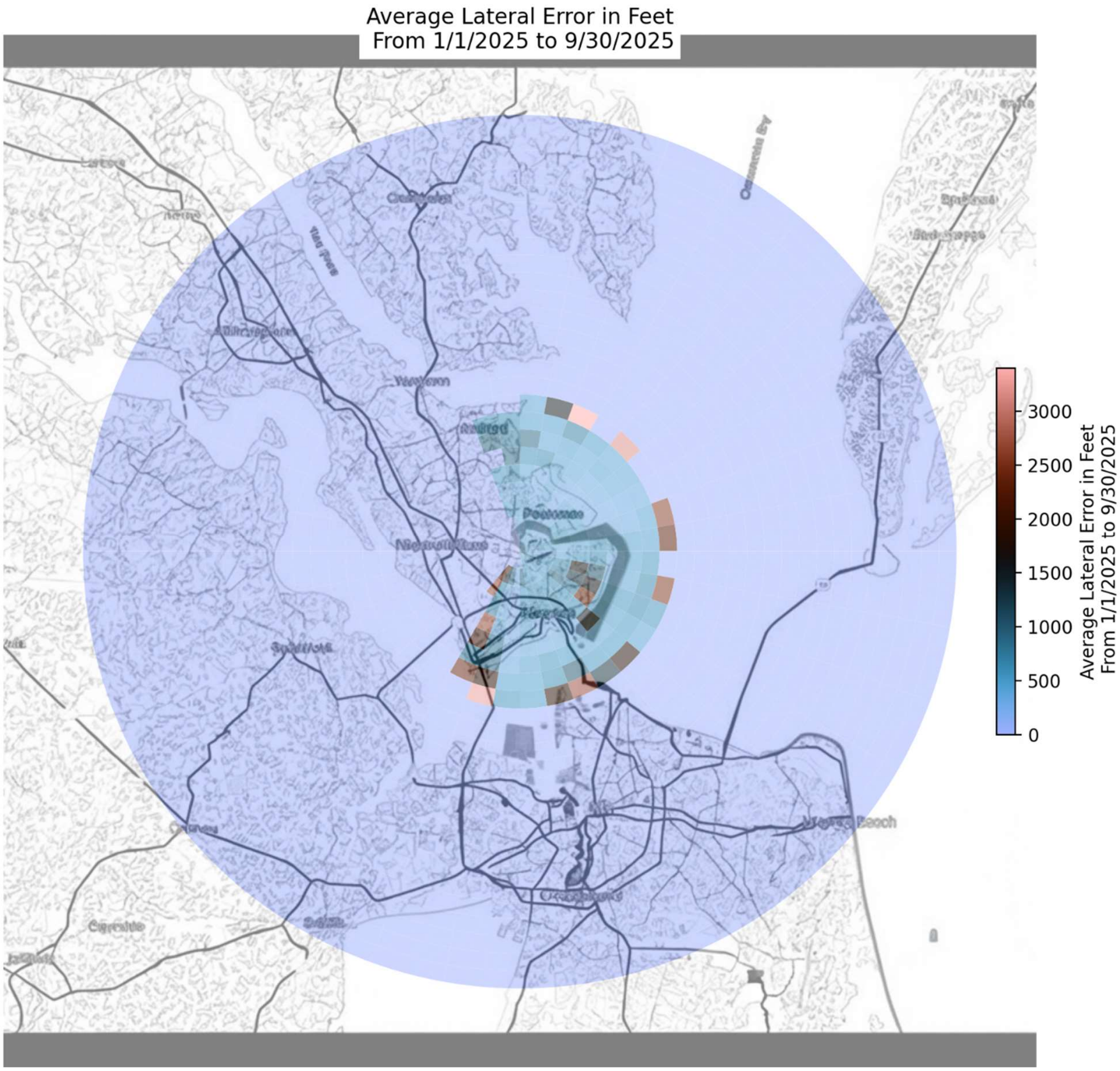
Average Lateral Error in Feet
From 1/1/2025 to 9/30/2025
3000
2500
2000
1500
1000
500
0
Average Lateral Error in Feet
From 1/1/2025 to 9/30/2025

Average Altitude Error in Feet
From 1/1/2025 to 9/30/2025

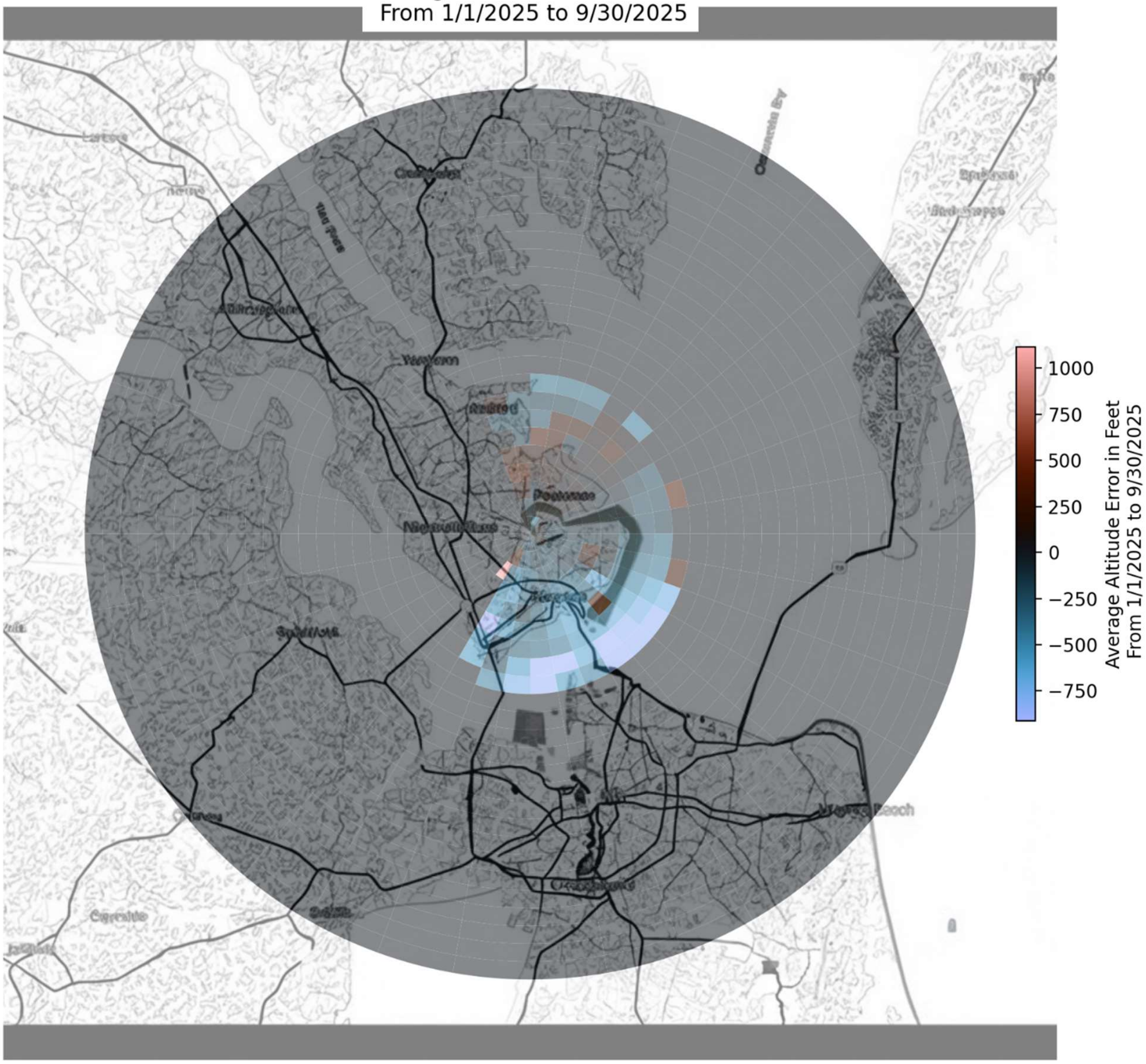

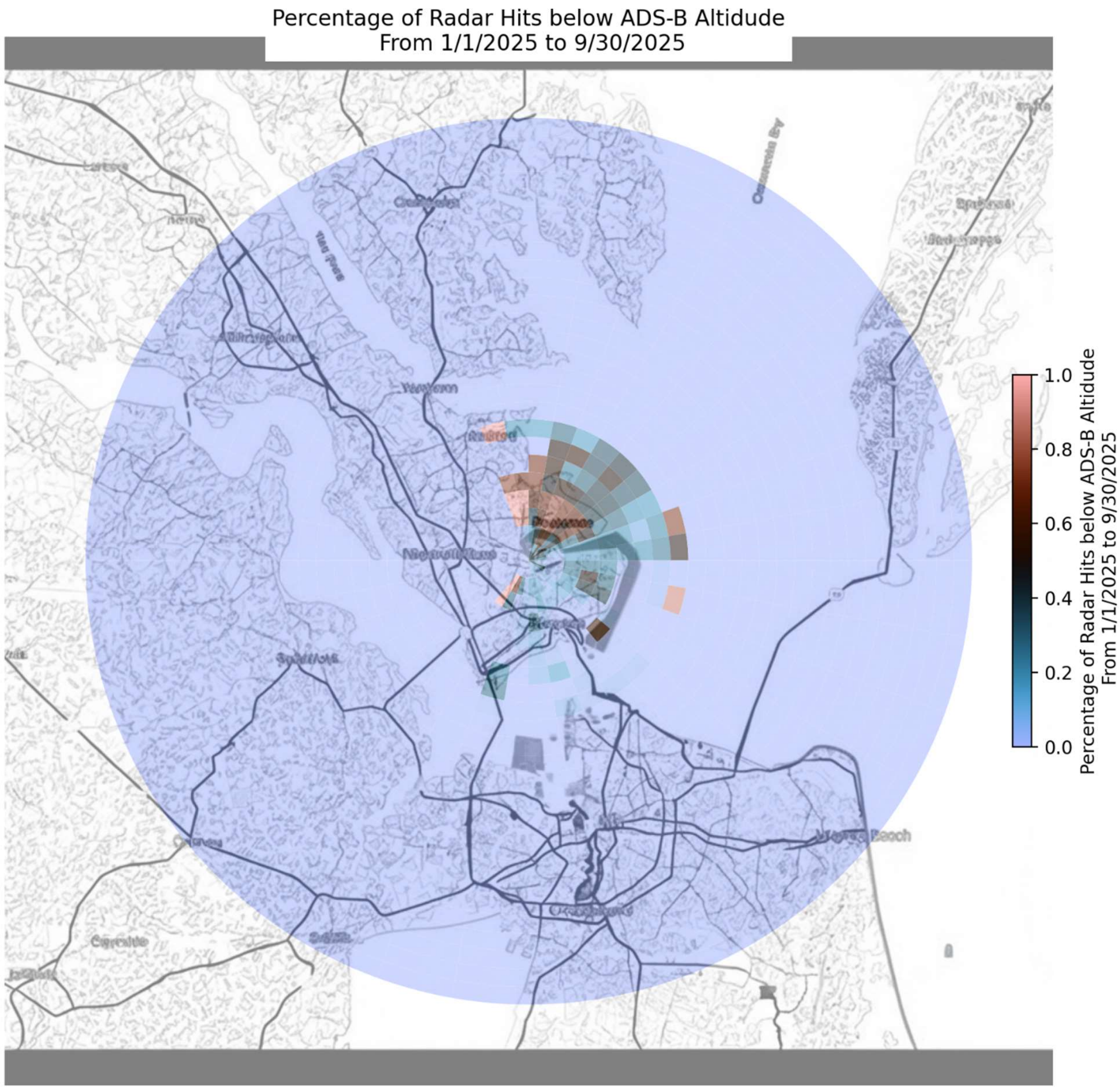
Percentage of Radar Hits below ADS-B Altidude
From 1/1/2025 to 9/30/2025
Percentage of Radar Hits below ADS-B Altidude
From 1/1/2025 to 9/30/2025
1.0
0.8
0.6
0.4
0.2
0.0